DISRUPTION OF TWO GENE LOCI PUTATIVELY ENCODING SIDEROPHORE-PRODUCING NONRIBOSOMAL PEPTIDE SYNTHETASES AND CHARACTERIZATION OF SIDEROPHORE MUTANTS

A Thesis

by

JAMES FRANKLIN HURLEY IV

Submitted to the Office of Graduate Studies of
Texas A&M University
in partial fulfillment of the requirements for the degree of

MASTER OF SCIENCE

December 2009

Major Subject: Plant Pathology

DISRUPTION OF TWO GENE LOCI PUTATIVELY ENCODING SIDEROPHORE-PRODUCING NONRIBOSOMAL PEPTIDE SYNTHETASES AND CHARACTERIZATION OF SIDEROPHORE MUTANTS

A Thesis

by

JAMES FRANKLIN HURLEY IV

Submitted to the Office of Graduate Studies of
Texas A&M University
in partial fulfillment of the requirements for the degree of

MASTER OF SCIENCE

Approved by:

Chair of Committee,	Charles M. Kenerley
Committee Members,	Deborah Bell-Pedersen
	Herman B. Scholthof
Head of Department,	Leland S. Pierson, III

December 2009

Major Subject: Plant Pathology

ABSTRACT

Disruption of Two Gene Loci Putatively Encoding Siderophore-Producing Nonribosomal Peptide Synthetases and Characterization of Siderophore Mutants.

(December 2009)

James Franklin Hurley IV, B.A., University of Colorado at Boulder

Chair of Advisory Committee: Dr. Charles M. Kenerley

The soil-borne, rhizosphere-competent, filamentous fungus *Trichoderma virens* is a well-known biocontrol agent able to control pathogenic fungi through the production of antibiotics, the induction of systemic resistance in host plants, or by directly parasitizing the competing fungus. Competition for iron is another means by which *Trichoderma* can hinder competing microorganisms, and siderophores are a means by which microorganisms obtain iron. *In silico* analysis of the *T. virens* genome suggested that two genes putatively encoding extracellular siderophore-producing nonribosomal peptide synthetases (NRPSs) were present.

In this study, a disruption was created in one of the genes, *TvNPS6*, to create a mutant unable to produce the NRPS TvNps6 (ΔTvnps6). Previously, a mutant (ΔTvsidD) had been generated with a disruption in the second gene (*TvSIDD*) encoding an NRPS thought to be involved in siderophore biosynthesis. A double mutant (ΔΔTvsidDTvnps6) was generated by transformation of a ΔTvsidD strain with a vector targeting disruption of *TvNPS6*. This resulted in transformants disrupted within both the

putative siderophore-producing NRPSs. Thus, three mutants were available for analysis of the role of these genes in the ecology of *T. virens*. Transformants were confirmed by PCR and Southern blotting analysis.

Phenotypic characterization of the mutants included both HPLC analysis of siderophore production, growth on agar and in liquid media, conidiation, germination in the presence of hydrogen peroxide, biocontrol against *Pythium ultimum*, *in vitro* confrontation against *Rhizoctonia solani* and growth with iron chelators to determine the contribution of reductive iron assimilation (RIA) compared to that of siderophores. The HPLC analysis demonstrated that *T. virens* Gv 29-8 (wild-type) produced a single siderophore peak when grown in an iron-depleted medium. This peak was not present in the ΔTvnps6 and ΔΔTvsidDTvnps6 mutants but was apparent with the ΔTvsidD mutants. From the HPLC analysis, *T. virens* evidently produces a coprogen-type siderophore. Few differences were observed in the other phenotypic tests, though hydrogen peroxide showed some small inhibitory effects towards the ΔTvnps6 mutants. The addition of chelators, which inhibit RIA, exerted some negative effects on all strains growing under iron-limited media, particularly the ΔTvnps6 and ΔΔTvsidDTvnps6 strains.

This study demonstrated that although *T. virens* has two genes putatively encoding siderophore producing NRPSs, only the *TvNPS6* gene was required for extracellular siderophore production. The greater sensitivity of the mutants towards the iron chelators suggests that unlike other other fungi studied, *Trichoderma virens* utilizes

RIA, rather than siderophore production, as the primary means by which the fungus obtains iron in an iron-limited environment.

ACKNOWLEDGEMENTS

I would like to thank Dr. R. Stipanovic and Dr. L. Puckhaber for their work on the HPLC analyses and identification of the siderophores.

My colleagues in the lab deserve thanks. To Frankie Crutcher and Natthiya Buensanteai, I am grateful for their advice considering their stronger molecular background as well as their sympathetic ear. Thanks to Cathy Kelton for setting up/performing many of the repetitions of the phenotypic experiments and maintaining a pleasant demeanor throughout. I appreciate David Laughlin's help setting up and performing the biocontrol experiments and wry humor. Thanks to Walter Vargas for his guidance during my first rotation through the lab. There were difficult days, but I was lucky to work in the Kenerley lab.

Dr. Prasun Mukherjee merits great thanks for his patience in instructing me in the rudiments of molecular biology and always making time to answer questions and address problems. Dr. Mukherjee is a scientist to be emulated- active and efficient in the lab, naturally curious, and cheerful in trying times.

I would like to express gratitude and appreciation to Dr. Charles Kenerley for taking me into his lab despite my inexperience and offering encouragement throughout my time at A&M. Dr. Kenerley was an invaluable source of no-nonsense answers and good conversation, and always had a knack for sensing how to keep motivation and morale high.

TABLE OF CONTENTS

Page

LIST OF FIGURES

FIGURE Page

LIST OF TABLES

1. INTRODUCTION

1.1. Biocontrol and Trichoderma

Biological control is the reduction of inoculum or disease-producing activity of a pathogen through biological agents other than humans (i.e. through their interventions) (Alabouvette et al., 2006). Four common mechanisms of biocontrol against fungal pathogens are parasitism, antibiosis, competition and induction of host resistance (Jeger et al., 2009). Parasitism involves the symbionts, or biocontrol agents (BCAs) parasitizing pathogenic fungi and thus reducing initial inoculum levels and subsequent disease severity. Although fungal BCAs' parasitism of pathogen hyphae is manifest, viral or viral-like BCAs may be subtly effective as they can induce hypovirulence in the pathogen (Alabouvette et al., 2006). Antibiosis is the production of secondary metabolites toxic or inhibitory to other microorganisms. Besides antibiotics, this category includes compounds such as cell wall degrading enzymes (CWDEs) essential for the aforementioned mycoparasitism. Competition is simply displacing the pathogen from the host substrate or outcompeting it for nutrients. For example, it has been observed that successful iron scavenging is one way mutualistic *Pseudomonas* species

---

This thesis follows the style of Fungal Genetics and Biology.

control fungal pathogens (Schippers et al., 1987). An indirect mechanism of biocontrol is the triggering of host induced systemic resistance (ISR). ISR occurs when a pathogenic or benign agent interacts with the plant in such a way that plant defenses are primed for subsequent challenges from disease-causing organisms. Following a cascade of molecular signals, there is increased production of phytoalexins and defense proteins, an "oxidative burst" of reactive oxygen species (ROS), and fortification of the cell wall (Djonović et al., 2006a; Van Loon, 2000).

Due to growing consumer health concerns and diminishing agronomic returns related to environmental degradation and development of resistant target organisms, purely chemical methods of controlling fungal pathogens are increasingly uneconomical (Vinale et al., 2008). There is heightened interest in biocontrol, but this method yields less consistent results than chemically-based approaches, mainly due to the pathogens' genetic variability circumventing the BCAs' specificity and unpredictable fluctuations in climatic conditions that may favor or inhibit components of the tripartite system (plant-symbiont-pathogen) to varying degrees (Vinale et al., 2008). Nevertheless, biocontrol appears more promising as the knowledge required to make this more complex system feasible is being gathered. For example, theoretical models have been formulated that suggest two key variables of biocontrol are the symbiont's rate of colonization and the length of time it remains active (Butt et al., 2001; Jeger et al., 2009). Biocontrol effectiveness is enhanced when used in tandem with cultural methods, such as crop rotation and soil solarization (Alabouvette et al., 2006). Determining the identities and functions of BCA secondary metabolites, as well as their fungal or bacterial producer's

optimal conditions for synthesizing these compounds, may allow selective application of these natural products in lieu of the entire organism, possibly assuaging public wariness towards these types of interventions, as well as lowering costs to the grower (Vinale et al., 2008). In addition, researchers have observed that BCAs like *Trichoderma* can be propagated and maintained for months on agrowaste materials like tea leaves or sawdust, further lowering the costs of obtaining adequate amounts of the BCA (Singh et al., 2007).

Trichoderma are commonly-occurring fungi found in soil and on the surface of roots. Although a few *Trichoderma* species have teleomorphic, or sexual, stages classified under the genus *Hypocrea*, sexual stages are generally unknown, and biocontrol strains are asexual (anamorphic) (Samuels, 2006). The (*in vitro*) life cycle of *Trichoderma* involves germination of conidia within 24 hours of inoculation, followed by visible colony expansion on the second and third days. Green conidia appear on the third or fourth day following inoculation (Kubicek and Harman, 1998).

Trichoderma species are opportunistic avirulent plant symbionts that are antagonistic towards many pathogenic fungi and beneficial to such diverse hosts as cotton, tomato, chickpea and peanut (Benitez et al., 2004: Singh et al., 2007). In 1989, *T. harzianum* was the first fungus registered with the EPA as a plant disease control agent (Fravel, 2008). *Trichoderma* species employ parasitism against pathogens (Chet and Baker, 1981), are prolific producers of secondary metabolites like CWDEs and antibiotics (Ghisalberti and Sivasithamparam, 1991), and are known to elicit induced systemic resistance (ISR) in their hosts (Yedida et al., 1999). They are rapid colonizers

due to fast growth and vigorous spore production (Vinale et al., 2008), and in addition can degrade such hazardous compounds as pesticides and hydrocarbons (Harman et al., 2004).

T. virens is a well-known biocontrol fungus (Howell, 2003). *T .virens* has straight phialides, a *Gliocladium*–like branching pattern, and grows optimally on PDA at 25° C with yellow or no pigmentation (Chaverri et al., 2001). Researchers have observed mycoparasitism, induced host resistance, and antibiosis generated by such secondary compounds as gliotoxin and gliovirin (Howell and Stipanovic, 1983). Howell et al. (1993) proposed dividing *T. virens* into "P" and "Q" classes according to these two natural products. The P strain produces gliovirin, which inhibits the fungal-like Oomycota, such as *Pythium*. The Q strain employs the broader spectrum antimicrobial compound gliotoxin. Other secondary compounds, including the mycoherbicide viridiol (Howell and Stipanovic, 1984; Jones et al., 1988) and peptaibols biosynthesized from nonribosomal peptide synthetases (NRPSs), have been described for this species (Wiest et al., 2002; Wei et al., 2005). A proteaceous elicitor, Sm1, from *T. virens* has been shown to trigger an oxidative burst and increased defense protein synthesis in the cotton host as well as eliciting ISR in maize (Djonović et al., 2007).

1.2. Iron acquisition

Iron is a required micronutrient for nearly all organisms. Since it can reversibly assume different valences, it is a key metabolic element that is involved in processes

such as electron transport, macromolecule synthesis, and respiration (Haas et al., 2008). It is an essential constituent of redox cofactors such as cytochrome P450, and is also a component of catalases and peroxidases, which reduce the harmful effects of the ROS hydrogen peroxide (H_2O_2) (Madigan and Martinko, 2006).

Although iron is the fourth most abundant element in the Earth's crust (5% by mass), bioavailability of iron is limited since ferrous [Fe^{2+}, or iron(II)] iron is readily oxidized by oxygen to ferric [Fe^{3+}, or iron(III)] iron hydroxides ($FeOH_3$), which are comparatively insoluble (10^{-17} M) at biological pH (roughly 7) (Schlesinger, 1997). However, more acidic environmental pH values reduce the degree to which ferric iron serves as a Lewis acid (electron pair acceptor); the associated water molecules are less likely to lose a proton and precipitate with iron as $FeOH_3$ (Kosman, 2003). Iron availability is further limited since ligands holding the predominant, more highly-charged ferric form are more difficult to displace than those holding divalent cations (Kosman, 2003). Competition from other species is also constant.

Fungi use both high-affinity and low-affinity systems to obtain iron. High- and low-affinity refers to the specificity of the mechanism, with the high-affinity systems having lower dissociation constants with their substrates (Philpott et al., 2006). Under iron-replete conditions, the model yeast *Saccharomyces cerevisiae* takes up iron through low-affinity transporters such as Fet4p and Smf1p (Dix et al., 1994). Low-affinity heme iron uptake has been observed in *Candida albicans* (Santos et al., 2003) and *Histoplasma capsulatum* (Foster, 2002). In addition to the low- and high-affinity systems, studies with *S. cerevisiae* has shown that excreted phenolic compounds (e.g.

anthranilate) can allow uptake through non-enzymatic reduction of ferric iron. *S. cerevisiae*, which produces no siderophores (see below), can also obtain iron by acidifying the environment with citric acid or other hydroxyl acids (Howard, 1999).

1.3. RIA, siderophores and siderophore synthesis

High-affinity systems are homeostatically controlled and expressed under iron-depleted conditions (Philpott, 2006). Fungi commonly employ two high-affinity pathways for iron uptake, reductive iron assimilation (RIA) and siderophores. With *Saccharomyces cerevisiae* serving as the paradigm, RIA, like low-affinity transport, requires initial reduction of iron(III) at the plasma membrane by ferric reductases (Fres). The exact reductant is unknown but NADPH has been proposed (Winkelmann, 2001). Subsequently, the ferrous iron is passed to a complex composed of a copper-dependent oxidase, Fet3, and an iron permease, Ftr1. Both these proteins are required for successful iron uptake as formation of this heterodimer seems necessary for proper trafficking to its plasma membrane location (Kosman, 2003). The ferrous iron is oxidized back to the iron(III) form by the oxidase, then passes through the transmembrane permease to reach the cytosol. An explanation offered for this apparent inefficiency is that ferric iron in the environment is bound to chelators and requires the ferrireductase to release it. However, since other divalent cations (Ca^{2+}, Mg^{2+}) utilize the same low-affinity system as iron (see above), oxidizing the ferrous iron back to the trivalent state increases the specificity and thus enhances uptake in iron-poor conditions (Howard, 1999). The mechanism by which

the iron passes through the permease is unresolved, but some researchers have conjectured that a thermodynamic gradient allows the iron (III) molecules to flow into the reducing interior of the cell (Winkelmann,2001) The RIA system can utilize various substrates, including iron salts, low-stability chelates such as ferric citrate, and siderophores (Haas, 2003).

Chelators (from the Greek work *chela*, meaning crab's claw) are agents, often organic, which form complexes with metal ions. Chelation is a common phenomenon. Porphyrin rings in hemoglobin and chlorophyll contain iron and magnesium, respectively. The efficacy of ion sequestration by chelators relates to the number of ligands (usually oxygen or nitrogen) available, called the coordination number. For example, on the basis of the Gibbs free energy equation ($\Delta G=\Delta H - T\Delta S$), the enthalpy change ($\Delta H$) of chelation by six unidentate molecules (coordination number=1) versus one hexadentate molecule (coordination number=6) is approximately equal. However, less entropy is lost (ΔS not as negative) when the hexadentate molecule chelates since fewer molecules are involved, giving a more negative ΔG value at the same temperature (T). This means there is greater energy released upon formation with the hexadentate ligand and that the reverse reaction is less likely, so the association between the single hexadentate ligand and metal chelate is stronger. Other factors giving the hexadentate chelator an advantage involve ring formation and solvation changes (Greenwood and Earnshaw, 1997).

Fungi and bacteria can produce siderophores, low-molecular mass, ferric-specific chelators, to obtain iron. Fungal siderophores are primarily di- or tri-

hydroxamates, tetradentate or hexadentate ligands utilizing both a carbonyl oxygen and an oxygen bound to an adjacent nitrogen (Philpott, 2006) to chelate ferric iron. The hydroxamic acid loses an H^+ from the nitrogen-bound oxygen, giving it a negative charge, while the carbonyl oxygen interacts with the ferric iron with its lone pairs of electrons (see Figure 1). Due to the high charge of the trivalent ions, hydroxamates chelate ferric iron and other ions (Ga^{3+}, Al^{3+}) strongly, with ferric iron's ionic radius providing the highest binding affinity. Another factor enhancing the binding affinity is the electron configuration in ferric iron's 3d orbitals, in which each orbital contains a single, unpaired electron. In this arrangement, most of the interaction energy is due to the negatively charged ligands and positively charged ferric ion. Another consequence is that the ferric iron is spherically symmetrical and has no required orientation for binding to the siderophore (Winkelmann, 2001).

There are four major families of hydroxamate siderophores (Haas et al., 2008) (see Figure 1): rhodotorulic acid, fusarinines, coprogens, and ferrichromes. Rhodotorulic acid, produced by basidiomycetes, is a dihydroxamate siderophore. Fusarinines are linear or cyclic trihydroxamates connected by ester bonds. Coprogens are trihydroxamates with both peptide and ester bonds. Fusarinines and coprogens are usually secreted (extracellular) siderophores. Ferrichromes are cyclic siderophores formed by three hydroxamates and three amino acids. Ferrichromes usually serve as storage (intracellular) siderophores, though they may be excreted in saprophytic fungi, such as *Aspergillus* and *Penicillium* (Winkelmann, 2007). Decaying plants and competing bacteria may release damaging hydrolases, proteases, lipases and esterases.

Ferrichromes lack ester bonds and are more resistant than the other families to exoenzymatic degradation (Winkelmann, 2007).

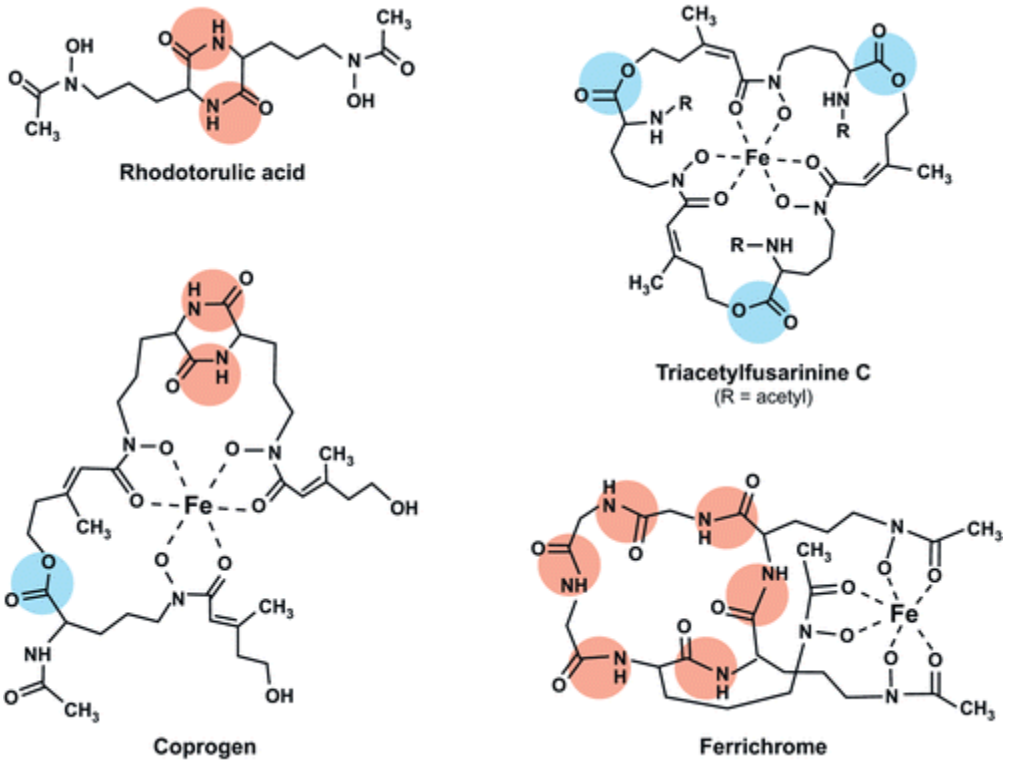

Fig. 1. Major siderophore families. Peptide bonds are highlighted in red, ester bonds are highlighted in blue (Haas et al., 2008)

Unlike low-affinity mechanisms, which can permit entry of other divalent cations such as copper and zinc (Hassett et al., 2000; Waters and Eide, 2002), the specificity of siderophore-chelate complex uptake through transporters is due to stereochemistry (Winkelmann,2001), i.e. the configuration and orientation of the complex and its binding

sites must perfectly complement that of the transporter. Notably, many fungi are able to exploit siderophores produced by other species (xenosiderophores). For example, *Aspergillus fumigatus* has a transporter similar to MirB of *A. nidulans*, suggesting an ability to process siderophores secreted by *A. nidulans* (Haas et al., 2008). The model organism *S. cerevisiae*, which produces no siderophores but is well-studied and serves as a general model for fungal iron uptake, can either reduce the ferric complex at the plasma membrane (RIA) or take up both the ligand (siderophore) and the bound iron and reduce it intracellularly (Philpott, 2006).

Most fungi produce both extracellular siderophores, which obtain iron from the environment, and intracellular siderophores, which are needed to store the iron. Iron not properly stored within the cell can react with hydrogen peroxide and form highly damaging hydroxyl radicals via the Fenton Reaction ($Fe^{2+} + H_2O_2 > Fe^{3+} + OH^- + OH\bullet$) (Halliwell and Gutteridge, 1984). Some research has suggested that siderophores are necessary for virulence (Oide et al., 2006; Lee et al., 2005; Hwang et al., 2008), whereas other investigators suggest that siderophores act as PAMPs (pathogen-associated molecular patterns) since their presence may elicit plant defenses against the fungus (Jones and Dangl, 2006; Liu et al., 2007). In human pathogens, siderophores are usually essential as iron is tightly bound by heme, ferritin, transferrin and lactoferrin (Schrettl et al., 2007).

For siderophore synthesis, Plattner and Diekmann (1994) proposed that the amino acid L-ornithine first undergoes hydroxylation then transacylation at the C5 nitrogen. Identification of the gene encoding the ornithine-N^5-monooxygenase, which

catalyzes the aforementioned first step, was achieved with *Ustilago maydis* (Mei et al., 1993). Orthologs to this gene, *SID1*, were subsequently identified in *Aspergillus* (*SIDA*) (Eisendle et al., 2003) and other ascomycetes. Mutation of this gene has been shown to completely block siderophore production in *Aspergillus, Ustilago* and *Fusarium* species (Haas et al., 2008); these mutants could be rescued with exogenous application of siderophores or ample ferrous iron. The latter implies low-affinity iron uptake is utilized (Eisendle et al., 2003; Haas et al., 2008). Genomic searches of *T. virens* and *T. reesei* revealed *SIDA* orthologs (Kenerley, unpublished). The second step, transacylation, produces hydroxamates (a CONOH group, a hydroxylamine next to a carbonyl group). The initial intermediate, N^5-hydroxy-ornithine, is acylated by various acyl-coenzyme A derivatives. The simplest derivative, acetyl-coenzyme A, leads to intracellular siderophore synthesis, whereas more complex molecules (such as anhydromevalonic acid) are used as the acyl groups to produce fusarinine monomers which can form extracellular siderophores. The third step (described in the next section) involves NRPSs covalently linking these acylated monomers through peptide or ester bonds to produce siderophores (Haas, 2008). A general overview is depicted in Figure 2.

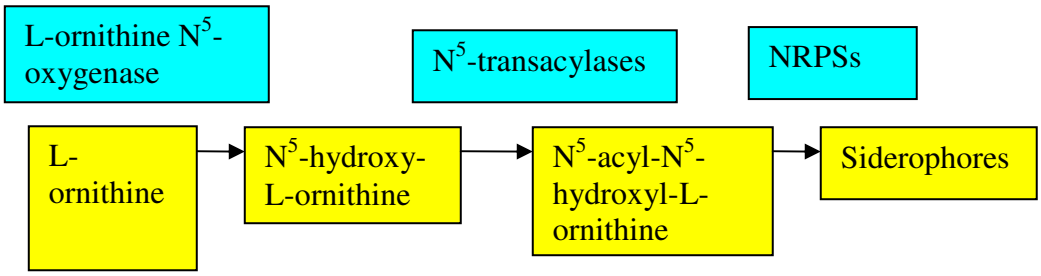

Fig. 2. General siderophore biosynthetic pathway (modified from Haas, 2008). Enzymes are in blue boxes, products are in yellow boxes.

1.4. Nonribosomal peptide synthetases

Nonribosomal peptide synthetases (NRPSs) link the hydroxamate products of the first two steps with peptide and/or ester bonds (Plattner and Diekmann, 1994). NRPSs are large, modular enzymes with multiple domains that play a prominent role in the production of secondary metabolites (Finking and Marahiel, 2004). One module adds a single amino acid to the growing peptide and contains an adenylation (A) domain for activation of the substrate, a peptidyl carrier protein (PCP, or thiolation, (T)) domain for attaching the activated substrate to the enzyme, and a condensation (C) domain that forms a peptide bond (Figure 3). A thioesterase (TE) domain terminates synthesis and releases the peptide from the NRPS, though it does not seem essential as it is absent from *Cochliobolus heterostrophus* and other filamentous fungi (Lee at al., 2005). In addition to the aforementioned domains, there may also be epimerization domains, cyclization domains and n-methylase domains. The epimerization domain changes the amino acid configuration from L to R and is distinct from ribosomal synthesis in which

only L- amino acids are used. The n-methylase and epimerization domains can lend durability to their products. Researchers have found that peptides formed by alternating D- and L-amino acids are more resistant to breakdown by proteases (Winkelmann et al., 2007). Since NRPSs can process a wide variety of substrates compared to the 20 amino acids from which ribosomes build peptides, NRPS products have great structural diversity. NRPSs have great potential for manipulation as excised modules still retain their enzymatic function and the A domain can be mutated to alter specificity. Since NRPS products include antibiotics and immunosuppressive factors, there is much promise for these enzymes in the medicinal applications (Finking and Marahiel, 2004).

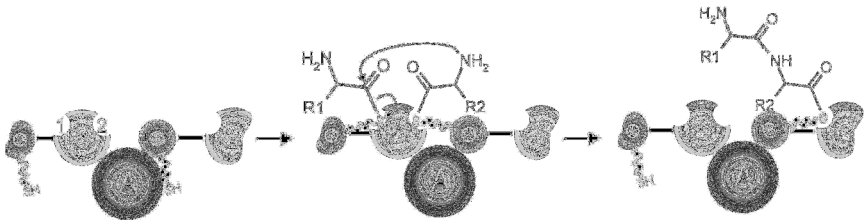

Fig. 3. Depiction of peptide production by NRPSs. Nucleophilic attack on the carbonyl carbon of amino acid 1(left) by the amine group of amino acid 2 releases amino acid 1from the sulfur atom of thiolation domain 1 and its condensation domain, elongating the peptide. A= adenylation domain, PCP (T)= peptidyl carrier protein (thiolation) domain, C= condensation domain. ©Annual Review of Microbiology, 58:453-488. (Finking and Marahiel, 2004)

The product of the NRPS Nps6 in *Cochliobolus heterostrophus* (Lee et al., 2005) has been identified and is proposed to have a role in virulence against maize and resistance to oxidative stress (Oide et al., 2006). All filamentous ascomycetes analyzed have orthologs to this NRPS (Haas et al., 2008). Evidence has been presented for two separate lineages within filamentous ascomycetes (Lee et al., 2005). The first lineage produces fusarinine-type siderophores and orthologs have been identified in *A. fumigatus* (Schrettl et al., 2007) and *F. graminearum* (Oide et al., 2006; Turgeon et al., 2007). The second group produces coprogen or coprogen derivative siderophores; orthologs have been identified in *Neurospora crassa* (Oide et al., 2006; Turgeon et al., 2007) and *Magnoporthe grisea* (Haas et al., 2008).

SIDD has been described as the gene encoding the NRPS (SidD) involved in the production of extracellular siderophores (Screttl et al., 2007), whereas *SIDC* encodes the NRPS (SidC) for intracellular siderophores [ferricrocin(FC) type]. *SIDD* was demonstrated to be essential for the production of fusarinine type siderophores in *A. fumigatus* (Schrettl et al., 2007). Fusarinine C is formed from three N^5-*cis*-anhydromevalonyl-N^5-hydroxyornithine (called *cis*-fusarinine) residues joined by ester bonds. Acetyl CoA can be joined to a fusarinine by N^2-acetylation to form triacetylfusarinine C (TAFC). In *A.fumigatus*, *SIDG* encodes the N^2-transacetylase. *SIDG* mutants cannot produce TAFC; as a result fusarinine C is the major siderophore. Research has shown that *SIDG* mutants have normal phenotypes, suggesting that fusarinine C can fully compensate for the loss of TAFC (Schrettl et al., 2007; Haas et al., 2008).

A coprogen-producing NRPS was first identified in *C. heterostrophus* (Lee et al., 2005), followed by identifications in *N. crassa*, *C. miyabeanus*, and *Alternaria brassicicola* (Oide et al., 2006; Turgeon et al., 2007). Lee et al., (2005) examined 11 genes that encode for NRPSs in *C. heterostrophus* and found that only the *NPS6* product was necessary for virulence against maize and had a role in protecting the fungus from oxidative stress, which is a common defense initiated by host plants (Mittler et al., 2004). A similar dependence on the Nps6 protein for resistance to oxidative stress and virulence of several fungal pathogens, including *C. miyabeanus* (rice), *F. graminearum* (wheat) and *A. brassicicola* (*Arabidopsis*) has been shown (Oide et al., 2006), as *NPS6* mutants under iron-depleted conditions were more susceptible to oxidative stress and showed reduced virulence to their respective host. Virulence could be rescued with exogenous application of either iron or both saturated and unsaturated siderophores. This latter point emphasizes that siderophores are necessary for iron acquisition by *C. heterostrophus*, rather than iron denial to the host (Oide et al., 2006). Supporting a proposed phylogeny of the *NPS6* genes (Lee et al., 2005, Oide et al. 2006) found that introduction of an *NPS6* ortholog from *N. crassa* into *C. heterostrophus* restored virulence to maize and tolerance to hydrogen peroxide.

1.5 Analysis of T. virens *genome and research direction*

Genomic analysis of the gene clusters containing *SIDD* and *NPS6* was performed earlier (Mukherjee, unpublished) and is shown in Figure 4. The genes comprising the clusters are listed in Tables 1 and 2.

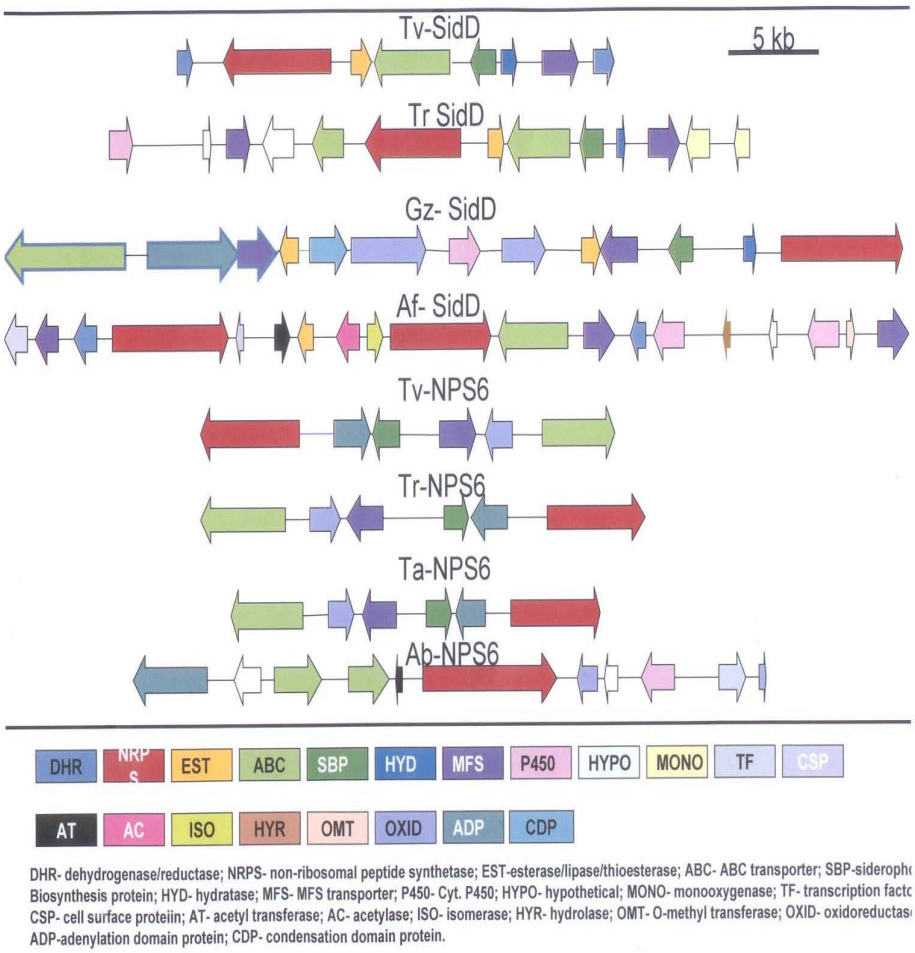

Fig. 4. Gene clusters containing *SIDD* (top) and *NPS6* (bottom). Ab= *Alternaria brassicicola* , Af= *Aspergillus fumigatus*, Gz= *Gibberella zeae***,** Tv=*Trichoderma virens* , Ta = *T. atroviride* ,Tr= *T. reesei* .

Table 1 Genes comprising homologous *SIDD* clusters. The NRPS row describes domains (A=adenylation, T=thiolation, C=condensation, dA=degenerate adenylation)

	Aspergillus fumigatus SidD	*Gibberella zeae* SidD	*Trichoderma virens* SidD	*Trichoderma reesei* SidD
NRPS	(2) SidDE + ATCdATC	ATCTC	ATCTC	ATCTC
ADP (Adenylation Domain Protein)	-	1	-	-
MFS (major facilitator superfamily) transporter	3	2	1	2
OXID (oxidoreductase)	-	2	-	-
ABC (transporter)	1	1	1	2
HYPO (hypothetical)	1	-	-	2
AT (acetyltransferase)	1	-	-	-
SBP (siderophore biosyn. protein)	-	1	1	1
TF (transcription factor)	1	-	-	-
P450 (cytochrome)	2	1	-	1
EST (esterase/lipase/thioesterase)	1	2	1	1
DHR (dehydrogenase/reductase)	2	-	2	-
HYD (hydratase)	-	1	1	1
MONO (monooxygenase)	-	-	-	2
CDP (condensation domain protein)	-	1	-	-
AC (acetylase)	1	-	-	-
ISO (isomerase)	1	-	-	-
OMT (O-methyl transferase)	1	-	-	-
HYR (hydrolase)	1	-	-	-
CSP (cell surface protein)	1	-	-	-
TOTAL=	19	13	8	13
Siderophore produced	Fusarinine C > TAFC	TAFC	None detected	?

Table 2 Genes comprising homologous *NPS6* clusters

	Alternaria brassicicola. NPS6	*Trichoderma virens* NPS6	*Trichoderma reesei* NPS6	*Trichoderma atroviride* NPS6
NRPS	ATCTTC	ATCT	ATCTC	ATCTC
ADP (Adenylation Domain Protein)	1	1	1	1
MFS (major facilitator superfamily) transporter	-	1	1	1
OXID (oxidoreductase)	2	1	1	1
ABC (transporter)	2	1	1	1
HYPO (hypothetical)	2	-	-	-
AT (acetyltransferase)	1	-	-	-
SBP (siderophore biosyn. protein)	-	1	1	1
TF (transcription factor)	1	-	-	-
P450 (cytochrome)	1	-	-	-
EST (esterase/lipase/thioesterase)	-	-	-	-
DHR (dehydrogenase/reductase)	-	-	-	-
HYD (hydratase)	-	-	-	-
MONO (monooxygenase)	-	-	-	-
CDP (condensation domain protein)	-	-	-	-
AC (acetylase)	-	-	-	-
ISO (isomerase)	-	-	-	-
OMT (O-methyl transferase)	-	-	-	-
HYR (hydrolase)	-	-	-	-
CSP (cell surface protein)	-	-	-	-
TOTAL=	11	6	6	6
Siderophore produced	Dimethyl-coprogen	Yes, I.D.?	?	?

Trichoderma virens appears to be unique in that two putative extracellular siderophore-producing NRPSs, designated TvSidD and TvNps6, are present. To confirm this, I proposed first to disrupt the *TvNPS6* gene in the wild-type strain (Gv29-8) of *T.virens* and in a ΔTvsidD strain to generate a double mutant (ΔΔTvsidDTvnps6) that should be unable to generate extracellular siderophores. After verification of the gene disruptions, various phenotypic assays were conducted to support the hypothesis that these two NRPSs are involved in siderophore production.

In summary, I hypothesized that the *SIDD* and *NPS6* orthologs of *T. virens* encode siderophore-producing NRPSs. Disruption of the genes will alter siderophore production and affect *Trichoderma* negatively due to iron-deficiency. Loss of the siderophore product was confirmed by HPLC analysis, whereas the aforementioned phenotypic assays detected the effects of the loss of NRPSs on various aspects of *T. virens* growth and development.

2. METHODS AND MATERIALS

2.1. Materials

2.1.1. Fungal materials

Two strains of *T. virens* were used in this study: the wild-type strain, Gv29-8, and an arginine-auxotrophic strain, Tv10-4, which was the recipient for transformation in the production of the double (2x) mutants. The arginine-auxotroph was created by a point mutation in the small subunit of a carbamoyl phosphate synthetase (*arg*2) after treatment with 4-nitroquinoline-1-oxide (NQO) (Baek and Kenerley, 1998). These strains were maintained on PDA. An isolate of the pathogen *Pythium ultimum* was provided by C. Howell (USDA-Agricultural Research Service, Southern Plains Agricultural Research Center, College Station, Texas). The *Rhizoctonia solani* pathogen was isolated from a diseased cotton seedling in a production field from College Station, Texas (Djonović et al., 2006b).

2.1.2. Growth media

The phenotypic experiments used variations of Vogels minimal medium (Vogel, 1956) with sucrose (VMS, containing 1.5% sucrose). As the experiments required different levels of iron, both VMS Fe+ (supplemented with 10µM ferrous sulfate

($FeSO_4$)) and VMS Fe- medium (no added iron) were prepared in iron-free glassware. Iron-free glassware was made by rinsing with water, soaking in 5% Extran (0.1% SDS) for 6-10 hours, soaking in 0.01% EDTA for 12-18 hours, rinsing with 1% HCl, followed by rinsing six times with double distilled water (ddH_2O). Normal VMS was used in some experiments and contains approximately 1.24μM of iron. Inoculum of *P. ultimum* used in the biocontrol assay was prepared by growing the pathogen in V8 broth for 10 days (Ayers et al., 1975). Wheat bran (5g wheat bran, 1g peat moss**,** 100mL H_2O, pH to 4.0) was inoculated with agar plugs of *R. solani*, and the pathogen was allowed to colonize the substrate for 10 days. The colonized wheat bran was air-dried, stored at 4°C, and used as inoculum for cotton seedling assays.

2.1.3. Hydroponics system

The hydroponics system, which was a prerequisite to the root colonization assay, largely followed the protocol of Djonović et al, 2007. The hydroponics system utilized mesh screens atop metal clamps placed in one-liter glass beakers containing approximately 300mL MS (Murashige and Skoog, Sigma) medium adjusted to pH 5.6. After being cleaned with 70% alcohol and 10% H_2O_2, 6-10 maize (inbred line B73) seedlings were placed in each chamber and shaken gently (approximately 20rpm). Meanwhile, the different strains (wild-type and mutants) were grown in VMS media. After three days, the hydroponics chambers were inoculated with approximately one gram of the *Trichoderma* mycelia.

2.2. Extraction of siderophores and HPLC analysis

2.2.1. Extraction of siderophores

The siderophore extraction protocol largely followed that of Oide *et al*., 2006. For quantitative analysis of siderophore production, 250mL flasks containing 100mL of VMS Fe- medium were inoculated with approximately 10^6 conidia. Cultures were then shaken for 72 hours at 125rpm on an orbital shaker. Mycelia were then removed by filtration, and culture filtrates were stored at -20 or -80°C prior to analysis.

To prepare filtrates for analysis, ferric chloride ($FeCl_3$) was added to the filtrates to a concentration of 1.5mM. A 1x18 inch glass column was loaded with 5ml sand, followed by 10mL Amberlite XAD-16. After tamping down the Amberlite, 15 more mL of sand was added. To pre-equilibrate the Amberlite, 20mL of 50mM KPO_4 buffer was eluted through the column.

The ferrated culture filtrates were loaded onto the column and eluted, with a pinkish-orange color indicating the presence of siderophores. To rinse the column of water-soluble compounds, two 20mL volumes of the KPO_4 were loaded and eluted. To remove buffer salts, two sequential 20mL volumes of mQ-H_2O were eluted. For both these rinses, the sidewalls of the column were also rinsed. A 40mL volume of methanol was loaded in the column to move the siderophores from the Amberlite into a 125mL flat-bottom boiling flask. The methanol was rotoevaporated from the siderophore solution at 30°C and reduced pressure. The remaining aqueous siderophore solution was

transferred to a 50mL boiling flask. The boiling flask was rinsed with a volume of ethanol equal to that of the siderophore solution transferred, so that the 50mL flask then contained double the volume of the siderophore solution initially transferred. The sample was rotoevaporated at 30°C and reduced pressure. This ethanol rotoevaporation step was repeated if the sample was not dry.

To dry the sample, 0.500mL of mQ-H_2O:acetonitrile (9:1) was added, swirling the flask to dissolve the siderophore residue on the walls. The siderophore solution was transferred to an HPLC vial. This process was repeated with a second volume of mQ-H_2O: acetonitrile, then the vial was sealed and submitted for HPLC analysis.

2.2.2. HPLC analysis

The HPLC analyses of siderophores were performed by the lab of Dr. R. Stipanovic of the Cotton Pathology Research Unit of the USDA Southern Plains Area Research Center based on the protocol of Zhang et al., 1993. The instruments used were an Agilent Technologies 1200 liquid chromatograph equipped with standard performance degasser, quaternary pump, autosampler, heated column compartment and diode array detector, along with a Hewlett-Packard 1050 liquid chromatograph quaternary pump and heated column compartment integrated with Agilent Technologies 1100 standard autosampler and diode array detector.

The analysis method involved maintaining a Phenomenex Prodigy ODS-3 5µm (4.6 x 250mm) column at 40°C. The mobile phase was a linear gradient of mQ-H_2O and

acetonitrile, with both containing 0.1% trifluoroacetic acid and run at 1.00 mL/minute. The gradient set points were 6% acetonitrile (0 min), 15% (10 min), 20% (15 min), 30% (20 min), 100% (26 min), 100% (29 min), 6% (30 min), and 6% (34 min). The chromatogram signals were at 254 nm and 435 nm (bandwidth 20nm), which were referenced to 550 nm (bandwidth 50nm). The spectra of the peaks were 210 to 600nm in 2.00 nm steps.

Solutions of authentic siderophores in mQ-H_2O:acetonitrile (9:1) were analyzed to provide information on their retention times and spectra in the HPLC systems. The standard compound solutions and their retention times are provided in Table 3. The solutions included 115µg/mL of triacetylfusarinine C, 122 µg/mL of a mix containing Fe-dimerum acid, neocoprogen II, linear fusigen, cyclic fusigen, neocoprogen I, coprogen and triacetylfusarinine C (both from EMC microcollections GmbH) and 173 µg/mL ferricrocin (kindly provided by Hubertus Haas of the Insbruck Medical University).

Table 3 Retention times for authentic siderophores in HPLC system

Siderophore	t_R (min)
Fe-dimerum acid	10.45
Ferricrocin	10.93
Neocoprogen II	12.30
linear & cyclic Fusigen	12.99
Neocoprogen I	13.18
Coprogen	15.57
Triacetylfusarinine C	22.96

2.2.3. Isolation of unknown compounds using HPLC

The method of isolation of unknown compounds from siderophore extracts using HPLC involved an Agilent Technologies 1200 liquid chromatograph equipped with standard performance degasser, quaternary pump, autosampler, heated column compartment and diode array detector with manual peak collection, as well as the Hewlett-Packard 1050 liquid chromatograph quaternary pump and heated column compartment integrated with Agilent Technologies 1100 standard autosampler and diode array detector with automated peak collection using an ISCO Foxy-200 x-y fraction collector.

The isolation method is just the analysis method described above but shortened as the peak of interest has a retention time of 12 minutes. Thus, a full run is not necessary. The column is a Phenomenex Prodigy ODS-3 5µm (4.6 x 250mm) maintained at 40°C. The mobile phase involves a linear gradient of mQ-H_2O and acetonitrile, both containing 0.1% trifluoroacetic acid and run at 1.00 mL/min. The gradient set points are 6% acetonitrile (0 min), 15% (10 min), 20% (15 min), 100% (16 min), 100% (19 min), 6% (20 min) and 6% (24 min). The chromatogram signals are 254 and 435 nm (bandwidth 20nm) referenced to 550nm (bandwidth 50nm). The spectra of peaks are 210 to 600nm in 2.00 nm steps.

2.3. Molecular analysis

2.3.1. Detection and disruption of NPS6 in T. virens

Using the *NPS6* sequence of *C. heterostrophus* (accession #AY884191), the *T. virens* ortholog, *TvNPS6*, was identified by a TBLASTN homology search in the Joint Gene Institute (JGI) *T. virens* genome portal (http://genome.jgi-psf.org/Trive1/Trive1.info.html). Two primers (Table 4) were designed from the nucleotide sequence of the *T. virens* ortholog to identify the 5' and 3' ends. The restriction sites Sal1 and Kpn1 were introduced into the forward, or Nps6f, (5'-GTTACCATGTCGACGGGTATCG-3') and reverse, or Nps6r, (5'-GTACTCGTCGAGATTGGTACCT-3') primers, respectively, to facilitate the cloning

of this fragment into the hygromycin resistance vector pATBS (Figure 5) (Mukherjee et al., 2003). This fragment is thought to encode parts of the first thiolation and condensation domain of the NRPS. The disruption will occur by inserting this fragment into genomic DNA by single crossover.

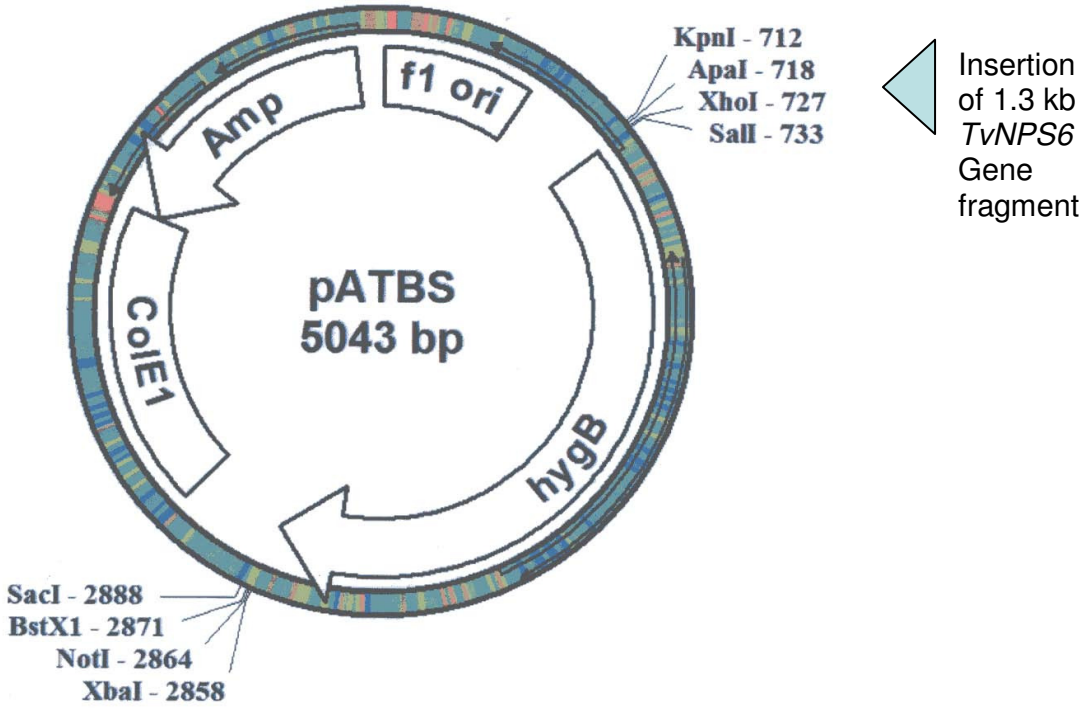

Fig. 5. The pATBS vector components and restriction sites. The insertion of the 1.3 kb *TvNPS6* gene fragment occurs between the Sal1 and Kpn1 sites and is marked with the blue triangle.

Table 4 Primers used in this study

Name	**Direction**	**Sequence 5' to 3'**	**T_m(°C)**
Nps6f	**F**	GTTACCATGTCGACGGGTATCG	57.3
Nps6r	**R**	GTACTCGTCGAGATTGGTACCT	55.6
OutS	**F**	GCATATGGACCATCTGAGTGTACC	57.0
OutAS	**R**	CTTAAACTGGTCCAGAGCTC	52.7
Hphforinv	**F**	GCACGAGATTCTTCGCCCTC	54.0
SidDf	**F**	GAACCTTGATAAAAACACGAAGAG C	54.7
SidDr	**R**	GGCATCATCTGTCTCACAAACG	56.2

Protoplasts for transformation of *T. virens* Gv 29-8 were prepared from 16 hour germlings grown in PDB (potato dextrose broth). To prepare protoplasts, approximately 10^8 conidia of Gv29-8 were inoculated into 100 mL of PDB and incubated for 16 hours at 25°C with shaking. Mycelia were harvested, washed with water, and 0.5g fresh weight was resuspended and digested in 2mL of mannitol osmoticum (50mM $CaCl_2$, 0.5M mannitol, and 50mM Mes/pH 5.5) containing 2.0 mg chitinase (0.2U/mg solid materials, Sigma, St. Louis,MO), 7.0 mg of lyticase (600 U/mg solid material, Sigma), and 44mg of cellulose "onozuka" R-10 (Housha Co., Tokyo, Japan). The mixture was incubated at

25°C with shaking at 200rpm for 30 minutes. Freshly formed protoplasts were diluted with 10mL of osmoticum, filtered through a 100-µm nylon mesh filter to retain undigested mycelia, centrifuged at 5400 rpm for 10 minutes, and the protoplast pellet was resuspended in osmoticum at approximately $5x10^7$ protoplasts/mL.

The transformation used a polyethylene glycol (PEG)-$CaCl_2$-mediated procedure (Thomas and Kenerley, 1989). To 240µL of competent fungal protoplast suspension, 5-10µg of vector in 20µL H_2O was added. The mixture was incubated on ice for 20 minutes followed by the addition 260µL of PEG solution [60% PEG3350 (Sigma, St. Louis, MO) in mannitol osmoticum] and further incubated for 20 minutes at room temperature. This suspension was mixed with the regeneration medium (PDAS; potato dextrose agar with 0.5M sucrose containing 50mg/L hygromycin B for selection) overlaid onto PDA regeneration plates and incubated at 28°C for 2-3 days and colonies transferred to PDA/hyg slants (50mg hygromycin B/L).

Transformants were screened by serial transfer to PDA (potato dextrose agar)/hygromycin slants (1µL hygromycin/4 mL media). Isolates able to sporulate on the PDA/hyg slants were further screened by transfer to a second PDA/hyg slant, followed by transfer to PDA slants, then a final PDA/hyg treatment. This serial transferring was adopted to select for stable transformants

Homologous recombination was verified by amplification using OutAS (5'-CTTAAACTGGTCCAGAGCTC -3'), and an inner primer, hphforinv, (5'-GCACGAGATTCTTCGCCCTC-3') from the hygromycin cassette. PCR conditions were 94° for 2 minutes, followed by 30 cycles of 94° 30 seconds, 55° 30 seconds, 72° 3

minutes, and then a 72° hold for 7 minutes. In this case, the presence of a 2.6 kb band indicated a successful disruption. Finally, single spore isolation was undertaken to separate the homologously recombined fungi from those that have ectopic insertions.

The absence of the wild-type copy was confirmed by using two primers, designated as OutS (5'- GCATATGGACCATCTGAGTGTACC -3') and OutAS (5'- CTTAAACTGGTCCAGAGCTC -3') that would amplify a region just outside the TvNPS6 sequence used for making the vector and would not amplify the gene if it is disrupted.

2.3.2. Southern blotting

Further confirmation of the disruption was obtained by Southern hybridization and HPLC analysis (see above) of siderophore production. Southern hybridization was performed with DNA extracted from the selected transformants, digested with Pst1, and probed with the 1.3kb [^{32}P]dCTP-labeled *TvNPS6* gene fragment. Digesting with the Pst1 restriction enzyme and hybridization yields two fragments (lengths 3.0 and 6.1kb) for *TvNPS6* mutants (ΔTvnps6).

2.3.3. Confirmation of ΔTvsidD

To reconfirm that the ΔTvsidD mutants still had the disruption before creating the double mutants, the mutants and WT were tested with the NPS6 forward and reverse primers and the SidD forward (5'-GAACCTTGATAAAAACACGAAGAGC-3') and reverse (5'-GGCATCATCTGTCTCACAAACG-3') primers. PCR conditions were 94° for 2 minutes, followed by 30 cycles of °94 30 seconds, 57° 30 seconds, 72° 1.5 minutes, then a 72° hold for 7 minutes. Amplification with the NPS6 primers will yield a 1.3 product, whereas amplification with the ΔTvsidD mutants will fail to produce a product.

2.3.4. Obtaining ΔΔTvnps6TvsidD double mutants

In addition to the *TvNPS6* mutant (ΔTvnps6), a double mutant (ΔΔTvnps6TvsidD*),* also referred to as "2x" or "DB") was created. This objective was simplified by the fact that a *TvSIDD* mutant (ΔTvsidD) had previously been constructed in the Kenerley lab. The gene was disrupted by insertion of an *argB* (arginine) gene into *TvSIDD* of an auxotrophic strain (Tv10.4) of *T. virens*. The procedure for creating the double mutant was the same as described above except that the protoplasts for transformations were from the ΔTvsidD mutant. The double mutants were confirmed by the same procedures described above, including Southern blotting.

2.4. Phenotypic characterizations

The phenotypic characterization included growth (both radial growth and dry weight), conidiation, germination inhibition by H_2O_2, confrontation against *Rhizoctonia solani*, root colonization of maize and biocontrol against *Pythium ultimum*. To ascertain the relative contributions of siderophores and RIA, wild-type *T. virens* was grown in media containing the ferrous iron chelator bathophenanthrolinedisulfonic acid (BPS).

2.4.1. Growth

Both radial growth and biomass were measured. For radial growth, 10µL of spore solution containing approximately 10^4 conidia was pipetted onto the center of a Petri dish containing 20mL of VMS Fe+ or Fe- agar. The plates were incubated at 27° C and area of mycelial growth was recorded daily by marking the circumference of the colony. The area was determined with ImageJ software. Moreover, growth on agar plates containing the ferrous iron chelator bathophenanthroline disulfonic acid (BPS) at a concentration of 100µM was determined.

To obtain biomass, 250mL flasks containing 100mL of Fe+ or Fe- medium were inoculated with 100µL of spore suspensions containing approximately 10^5 conidia. The cultures were shaken at 125rpm. On the third day, the mycelia were harvested, blotted dry, and then placed in a drying oven at 70°C for 24+ hours. Following drying, weights

were recorded after allowing the dried mycelia to sit for two hours to equilibrate to room humidity.

Two chelators, BPS and 2,2'-dipyridyl (2DP) were tested with Gv29-8. Six liquid media treatments were performed for each of the two trials: Fe-, Fe- with chelator, Fe+1mM $FeSO_4$, Fe+1mM $FeSO_4$ with chelator, Fe+10mM $FeSO_4$, and Fe+10mM $FeSO_4$ with chelator. Chelators were added to a concentration of 100µM. 250mL flasks containing 100mL of the respective media were inoculated with approximately 10^6 conidia and shaken at 125rpm on an orbital shaker for 72 hours. Following the incubation period, mycelia were harvested by filtration on pre-weighed filter papers. After drying for at least 24 hours at 80°C, weights were recorded.

2.3.2. Conidiation and germination

For conidiation assays, 100 µL of spore suspension containing approximately 10^6 conidia was pipetted and evenly spread on Fe+, Fe-, Fe+ 2 mM H_2O_2 and Fe- 2mM H_2O_2 agar plates. Plates were incubated for four days at 27°C. Following incubation, three 7.62mm (0.3 inch) diameter cores were removed from each plate, placed in 5 mL of 0.1% Tween aqueous solution, vortexed for 10 seconds, then conidia counted with a hemacytometer.

For germination inhibition by hydrogen peroxide, VMS plates were prepared containing 0 mM, 2 mM, and 5 mM H_2O_2. Spore suspension of 100µL containing approximately 100 conidia was spread evenly onto the 0 mM H_2O_2 plates, whereas

100µL of spore suspension containing approximately 1000 conidia was spread evenly on the 2 mM and 5 mM H_2O_2 plates. On the second day, the percentage germination of the different strains on the 0 mM plates was determined. On the third day, the percentage germination on the 2 mM and 5 mM plates was determined. This latter percentage was divided by the percentage germination on the 0 mM plates to calculate H_2O_2 inhibition for the different strains. This method eliminates discrepancies in the conidial concentrations of different spore suspensions.

2.3.3. Confrontation, biocontrol and root colonization

Confrontation assays against *R. solani* were conducted by placing cores of *R. solani* and *T.virens* on opposite ends of VMS Fe+ or VMS Fe- plates. The time required for *Trichoderma* to completely overgrow *Rhizoctonia* and reach the opposite edge of the plate was recorded and mycoparasitic coiling by *Trichoderma* was confirmed by microscopy.

Biocontrol was tested against *P. ultimum* with cotton as the host. Seeds were surface-sterilized by soaking for five minutes in 70% ethanol, followed by a two hour treatment in 10% H_2O_2. Thirty seeds were placed in a 50mL tube (Falcon), to which 510µL of latex were added, followed by vortexing. The coated seeds were allowed to dry for five minutes. These seeds were then added to a tube containing 0.3 grams of *T. virens* chlamydospores (ground and sifted through a 40 mesh filter), which was then vortexed. The pathogen inoculum was prepared by harvesting a 10-day-old culture of *P. ultimum*

from one plate of V8 broth. The entire contents were blended (Waring blender, high-speed setting for 30 seconds) and the slurry brought to a total of 100mL by the addition of sterile water. Soil was prepared by adding this 100mL of aqueous *Pythium* solution to 1000g of soil then mixing well with an electrical egg beater. Approximately 10 grams of soil and one treated seed were added to each medium-sized glass test tube. The positive controls contained *Pythium* but no *Trichoderma*, whereas the negative control lacked both *Pythium* and *Trichoderma*. The tubes were then incubated in a growth chamber at 28°C. After seven days, the cotton seedlings were rated on a scale of 1 to 3, with 1=healthy, 2= diseased, and 3= dead.

Root colonization was determined from corn plants grown in a hydroponics system. After three days of incubation in the hydroponics chamber, each set of seedlings was inoculated with approximately one gram of mycelia from the appropriate fungal strain. The seedlings were removed from the hydroponics system after two additional days of incubation and the roots were excised from the plant. The roots were rinsed with tap water to remove the fungal inoculum loosely associated with the roots. The roots were then submerged in a 1% NaClO treatment for 2 minutes, followed by 3x3 minute rinses with sterile ddH_20. Roots were then plated on media composed of modified GVSM lacking gliotoxin (Park et al., 1992). Following 48 hours of incubation at 27°C, the number of *Trichoderma* colonies was determined for the total root length to derive the colonies/cm value, the measure of root colonization.

2.3.4. Statistics

Statistics were conducted using the SAS Stat View program, with the Fisher Protected Least Significant Difference indicating statistical significance (p-value < 0.05) with 95% confidence. Graphs were created on Microsoft Excel. Experiments were performed with three replications unless stated otherwise.

3. RESULTS

3.1. HPLC analyses after mutant construction

HPLC of culture filtrates allows detection of siderophores. Chromatograms of the HPLC of the filtrates are shown in Figures 6-10. No siderophores were detected in the Fe+ medium filtrate for any strains assayed. For wild-type, growth in an iron-depleted medium yielded a compound at absorbance 12.7 minutes (x-axis), possibly corresponding to a coprogen-type siderophore (Figure 6). The ΔTvsidD mutant showed identical peaks to wild-type (Figure 7). This peak was absent in both ΔTvnps6 and double mutants grown in Fe- medium (Figures 8 and 9). To rule out the possibility that *TvSIDD* codes for an NRPS that produces an intracellular siderophore, mycelia were extracted and the supernatant submitted for analysis. There were no differences between the wild-type and ΔTvsidD intracellular extracts; both had the ferricrocin peak at 10.9 minutes (Figure 10).

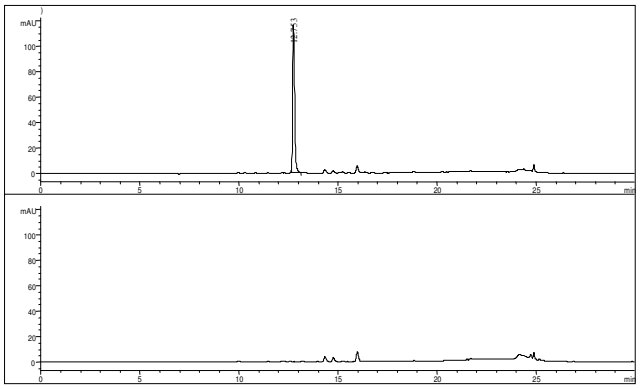

Fig. 6. HPLC profile for Gv29-8. Culture filtrate from fungi grown under iron-depleted (top) and iron-replete (bottom) conditions. The extract was injected in 10µL aliquots. The y-axis shows absorption and the x-axis shows retention times in minutes. The large peak at approximately 12.7 minutes retention time is for an extracellular coprogen-family siderophore.

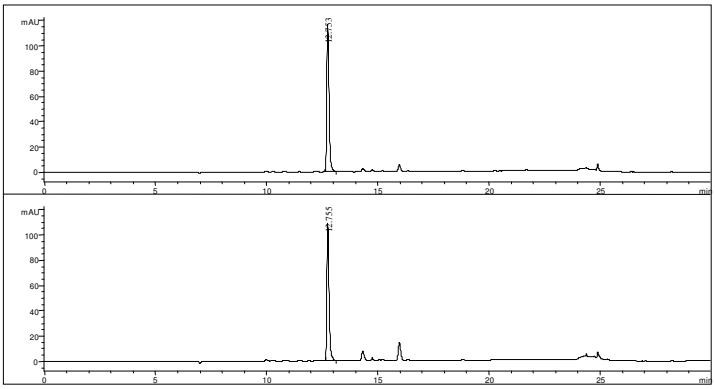

Fig. 7. HPLC analysis of Gv29-8 (top) and ΔTvsidD (bottom). Strains were grown in iron-depleted medium. The extract was injected in 10µL aliquots. The y-axis shows absorption and the x-axis shows retention times in minutes. The large peak at 12.7 minutes for both strains is for an extracellular coprogen-family siderophore.

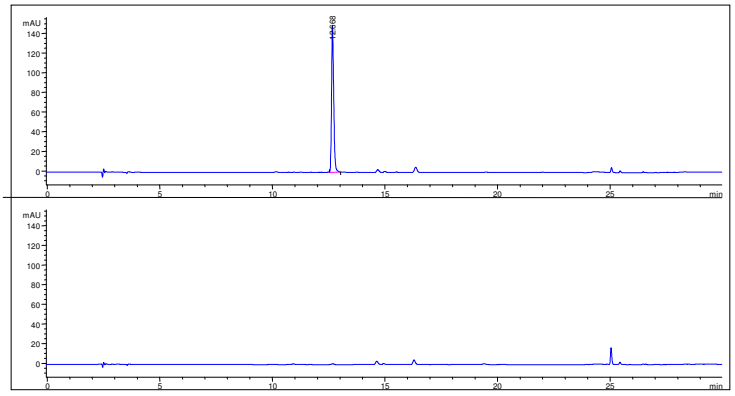

Fig. 8. HPLC analysis of Gv29-8 (top) and ΔTvnps4 (bottom). Culture filtrates from iron-depleted conditions. The extract was injected in 10µL aliquots. The y-axis shows absorption and the x-axis shows retention times in minutes. The ΔTvnps4 mutant lacks a peak at a retention time of 12.7 minutes corresponding to a coprogen-family siderophore.

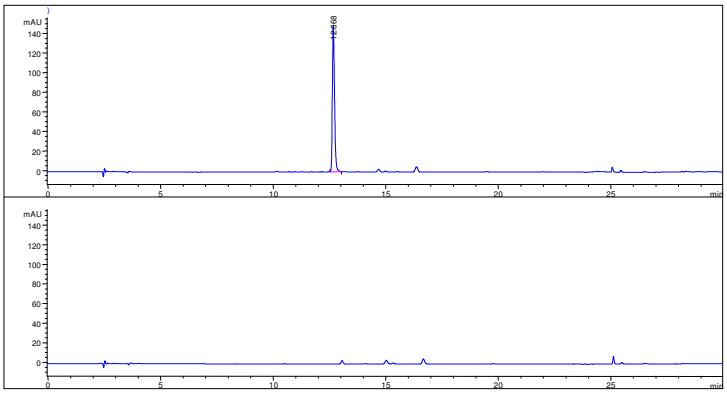

Fig. 9. HPLC analysis of Gv29-8 (top) and ΔΔTvsidDTvnps4 (bottom). Culture filtrates from iron-depleted conditions. The extract was injected in 10µL aliquots. The y-axis shows absorption and the x-axis shows retention times in minutes. Gv29-8 displays a peak at 12.7 minutes corresponding to a coprogen-family siderophore that the double mutant lacks.

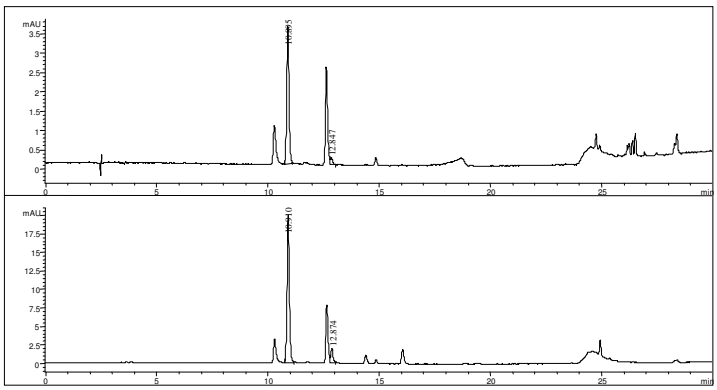

Fig. 10. HPLC analysis for presence of the intracellular siderophore ferricrocin. From mycelia of Gv29-8 (top) and ΔTvsidD-4 (bottom) grown in iron-depleted conditions. The extract was injected in 10µL aliquots. The arrow indicates a peak at 10.9 minutes retention time corresponding to the intracellular siderophore ferricrocin.

3.2. Detection and confirmation of mutant strains

3.2.1. Mutants of TvNPS6

Numerous checks were conducted to ensure the target *NPS6* gene was disrupted. Following transformation and screening on PDA/hygromycin, 103 out of 235 (44%) of the isolates were found to grow and sporulate after the multiple rounds of PDA/hygromycin. Eighteen of these potential transformants were assayed for gene disruption by PCR analysis. Three mutants were identified by PCR analysis for *TvNPS6*: designated ΔTvnps4, ΔTvnps15, ΔTvnps16. The amplified sequence (2.6kb, using OutAS and hphforinv primers, Table 4) is only present in DNA containing the hygromycin insert, so DNA without the insert does not yield a fragment (Figures 11 and 12).

PCR analysis using primers (OutS and OutAS, Table 4) located just outside the *TvNPS* sequence was also performed with putative transformants #4, 15, and 16. In this latter test, lack of a product occurs as the size of the fragment to be amplified by this primer set in the mutants is too large (approximately 8.6kb) for amplification by traditional PCR methods. The genomic DNA control and putative transformants lacking the insert demonstrate a band of 2.3kb. Use of the Nps6f and Nps6r primer sets results in a 1.3kb product in both the transformants and the genomic DNA (Figure 13).

3.2.2. Mutants of TvSIDD

The ΔTvsidD mutants, which were created prior to my project (Kenerley, unpublished), were reconfirmed. These mutants were generated in the auxotrophic strain Tv10.4 which is mutated in the gene encoding the small subunit of carbomoyl phosphate synthetases (Baek and Kenerley, 1998). Selected mutants were verified by PCR analysis using both the SidD primer set (SidDf/SidDr) and the Nps6 primer set (Nps6f/Nps6r) (Table 4). No product should be present in mutants when DNA is amplified with the SidD primer set as a portion of the gene has been replaced with the selectable marker (*arg2* gene). The Nps6 primer set results in a 1.3kb fragment in all strains (Figure 14). Homologous insertions were confirmed for ΔTvsidD designated ΔTvsidD4, ΔTvsidD46, and ΔTvsidD75 (see Figure 14).

3.2.3. Double mutants

Using the same protocol as described for the ΔTvnps6 mutants, a disruption in TvNPS6 was also generated in a ΔTvsidD background, yielding double mutants (ΔΔTvsidDTvnps6, also referred to as "DB" or "2x") designated ΔΔTvsidDTvnps4, ΔΔTvsidDTvnps5, ΔΔTvsidDTvnps9, ΔΔTvsidDTvnps10) (Figure 15). Use of the OutS and OutAS primer set does not produce a product as the fragment to be amplified is too large for amplification by standard PCR methods.

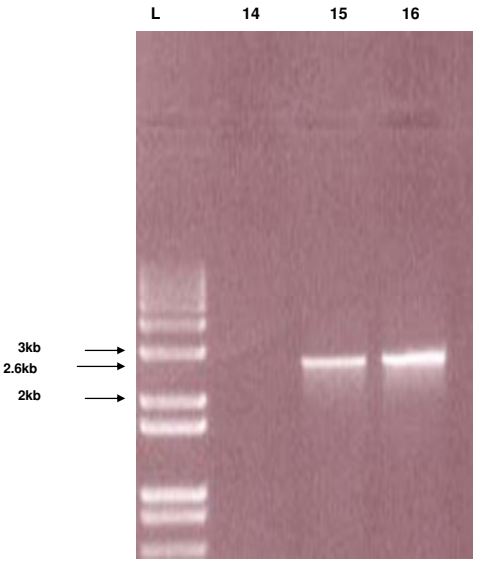

Fig. 11. Confirmation of disruption in transformants ΔTvnps15 and ΔTvnps16. Amplification with Hphforinv and OutAS primers (Table4) yields a fragment of approximately 2.6kb in strains disrupted in *TvNPS6.* Lanes from left to right: ladder (1 kb plus DNA), transformants 14,15,16.

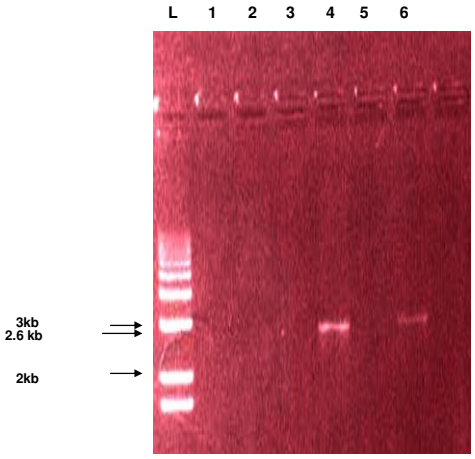

Fig. 12. Confirmation of disruption in transformant ΔTvnps4. Amplification of DNA with primer set Hphforinv/OutAS (Table 4). Appearance of 2.6kb fragment which includes the hygromycin insert is confirmation of disruption of the gene. Lanes from left to right: ladder, putative transformants 1 through 6.

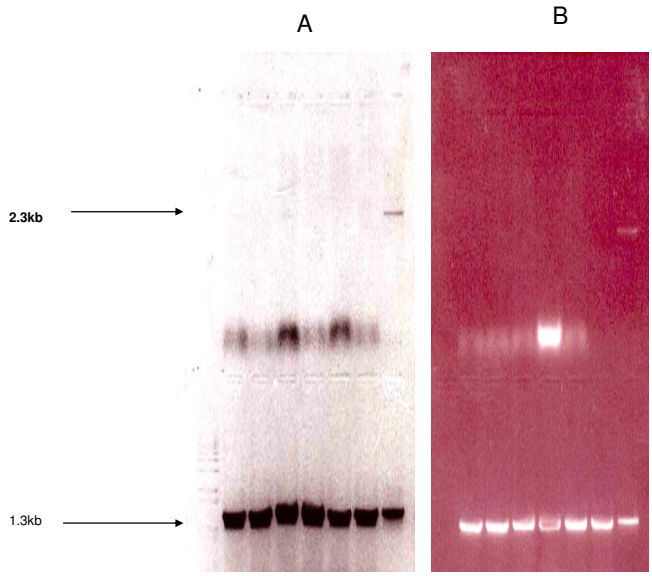

Fig. 13. PCR analysis of putative ΔTvnps6 transformants. OutAS/OutS (top) and Nps6f/Nps6r (bottom) primer sets (Table 4) were used. Lack of a product in the top of the gel indicates successful disruption (see page 48). For gel A (left), lanes contain, left to right, ladder,4,4,4,4,15,15, genomic DNA control; for gel B (right), lanes contain, left to right, ladder,15,15,16,16,16,16, genomic DNA control. The Nps6f/Nps6r primer set is a control primer pair for determining DNA quality. All isolates including WT should exhibit a product.

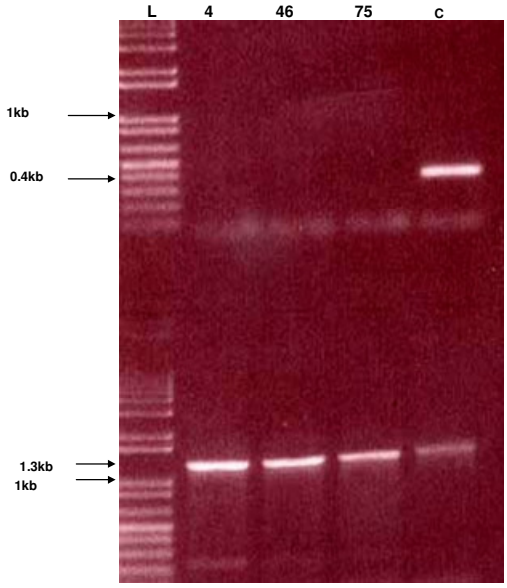

Fig. 14. Verification of ΔTvsidD disruption. The SidD primer set (top) was used. The Nps6 primer set was used to demonstrate an intact *TvNPS6* gene (bottom). Depicted, from left to right, are size standard, ΔTvsidD 4, 46, 75 and genomic DNA.

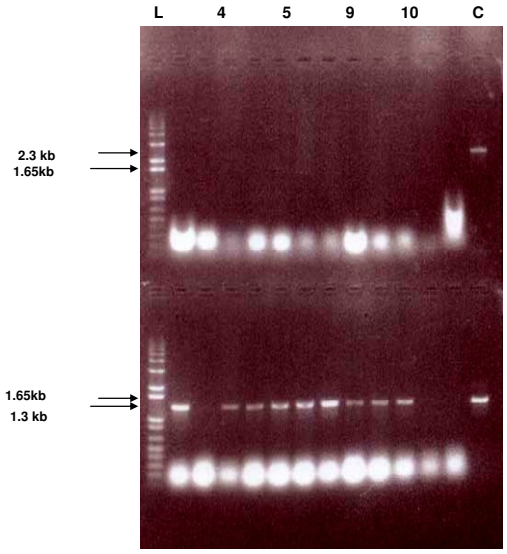

Fig. 15. PCR verification of ΔΔTvsidDTvnps6 mutants. In the top of the gel, amplification of double mutants with OutS/OutAS primer set (Table 4) does not result in a product. In the bottom half, the transformants and the genomic DNA produce a 1.3 kb product when amplified by the primer set Nps6f/Nps6r (Table 4). Lanes contain, from left to right, ladder, 4,4,4,5,5,5,9,9,9, 10,10,10, control.

3.2.4. Southern blotting

As the Pst1 restriction enzyme cuts within the insertion (Figure 16), Southern blot analysis provided further verification of the aforementioned ΔTvnps6 and ΔΔTvsidDTvnps6 mutants (Figures 17 and 18). Thus, mutant strains containing the transforming vector produce fragments of 3.0 and 6.1kb, whereas wild-type DNA yielded a single fragment of 2.8kb when hybridized with a 1.3kb probe from module one (Figure 16). The 6.1 kb fragment contains the *TvNPS6* fragment, the Bluescript vector, and part of the hygromycin resistance gene. The 3.0 kb fragment contains the second copy of the *TvNPS6* fragment and the portion of the hygromycin gene not in the 6.1 kb fragment (Figure 16). The same probe and process worked for Southern blotting both the *TvNPS6* mutants and the double mutants.

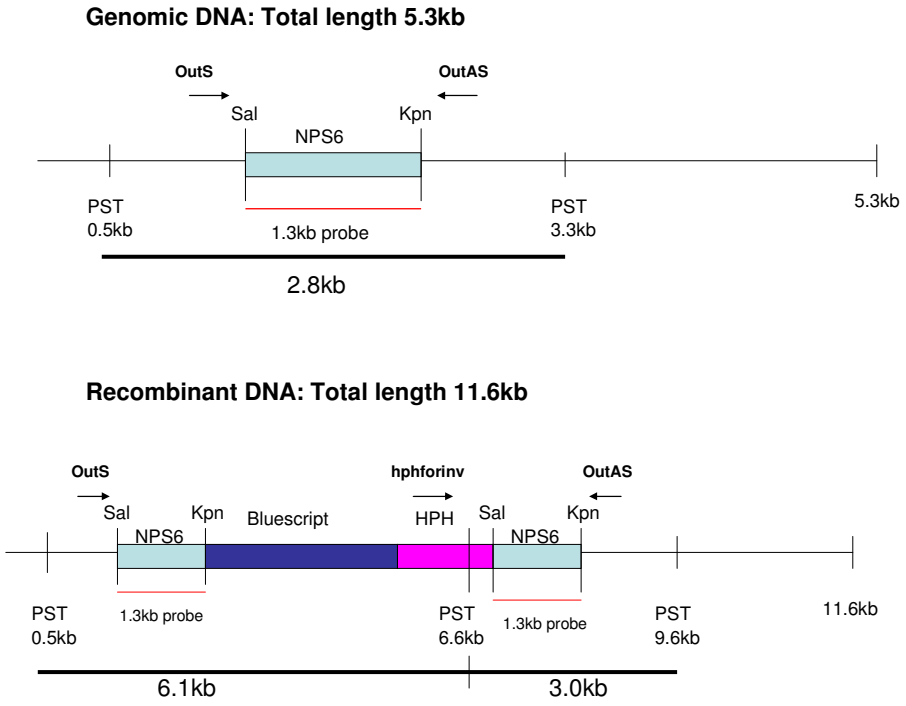

Fig. 16. Depiction of genomic and recombinant DNA with restriction sites. The probe is the 1.3kb section of NPS6 labeled with ^{35}P. An extra Pst1 site is present in the recombinant DNA**,** so it will yield two bands of lengths 6.1 and 3.0 kb. Wild-type will have a single 2.8kb band. Primer pairs are indicated above the restriction enzyme sites (see Table 4).

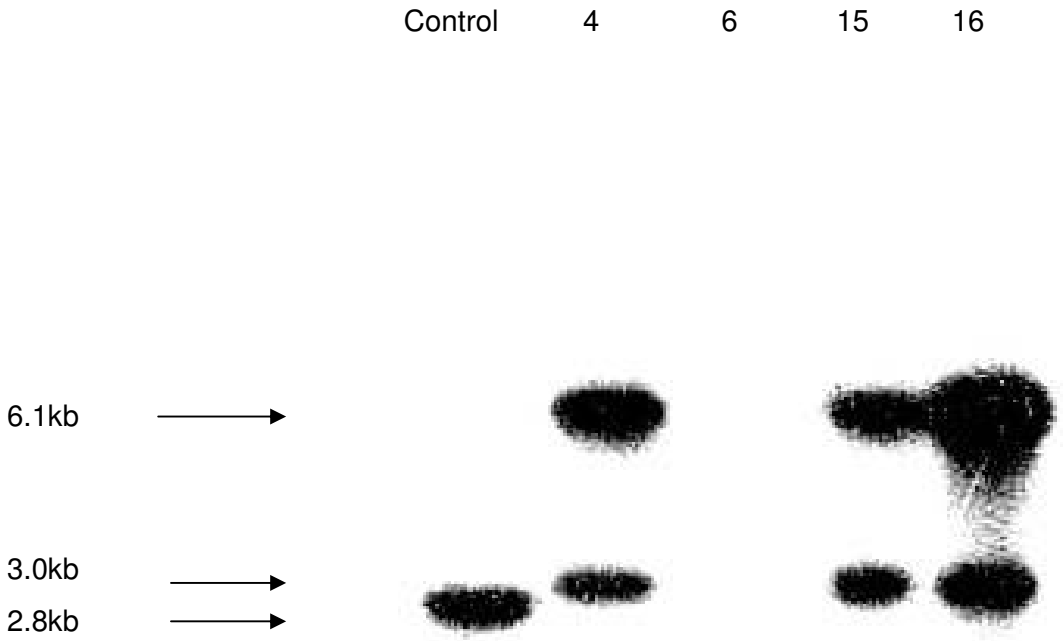

Fig. 17. Southern analysis and confirmation of ΔTvnps6 disruptants. The Pst1 restriction enzyme cuts within the insertion, producing two fragments of 6.1 and 3.0kb. Genomic DNA has a single 2.8kb fragment. Depicted from left to right, are wild-type DNA, ΔTvnps4, ΔTvnps6, ΔTvnps15, ΔTvnps16. The probe was a 1.3kb [^{32}P]dCTP-labeled *TvNPS6* gene fragment.

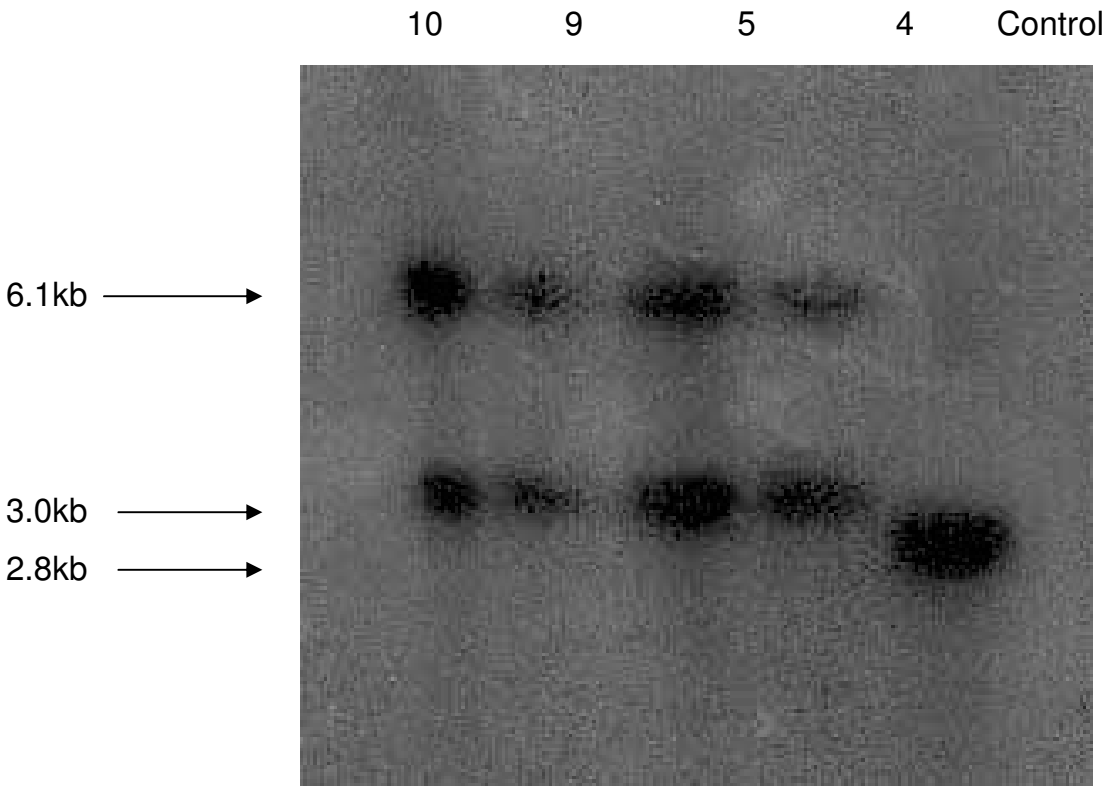

Fig. 18. Southern analysis and confirmation of double mutants. The probe was a 1.3kb [^{32}P]dCTP-labeled *TvNPS6* gene fragment. As with the ΔTvnps6 mutants (Fig.17), restriction digest with Pst produces two fragments for the mutants and a single fragment for wild-type DNA. Depicted from left to right are ΔΔTvsidDTvnps10, ΔΔTvsidDTvnps9, ΔΔTvsidDTvnps5, ΔΔTvsidDTvnps4 and genomic DNA.

3.3. Phenotypic experiments

3.3.1. Growth

Area of mycelial growth at 60 hours for wild-type and mutant strains is presented in Figure 19. The growth of strains was assessed on VMS Fe+ and VMS Fe- media, following inoculation of the center of the plate with conidia. Wild-type growth is significantly less than all ΔTvsidD and ΔTvnps6 for both treatments. Wild-type growth is significantly less than ΔΔTvsidDTvnps4 and ΔΔTvsidDTvnps10 for both treatments, but there is no significant difference between wild-type and ΔΔTvsidDTvnps9 for either treatment.

Biomass (represented by dry weights) of strains grown in VMS Fe+ and VMS Fe- liquid media following 3 days of incubation is presented in Figure 20. For the Fe+ treatment, wild-type growth was significantly less than both ΔTvnps6 mutant strains, but greater than ΔΔTvsidDTvnps5 and ΔΔTvsidDTvnps10. For the Fe- treatment, wild-type was likewise significantly less than both ΔTvnps6 mutants but greater than ΔΔTvsidDTvnps5 only.

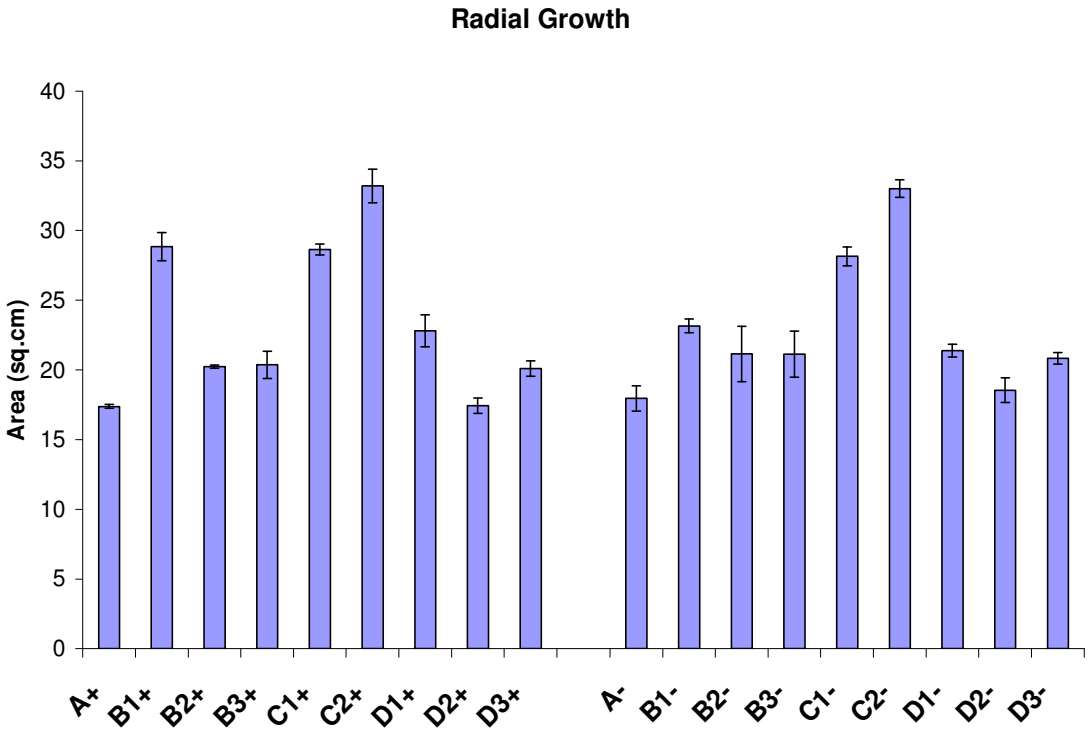

Fig. 19. Radial growth of WT (Gv29-8) and mutant strains. Growth was on Fe+ and Fe- agar medium. A=WT, B=ΔTvsidD (Mutants: 1=#4, 2=#46, 3=#75), C=ΔTvnps6 (Mutants: 1=#4, 2=#16), D=ΔΔTvsidDTvnps6 (Mutants: 1=#5, 2=#9, 3=#10).“+” and “-” signify VMS Fe+ and VMS Fe- media. Bars represent average area in mm^2 of three repetitions, and standard error represented by error bars.

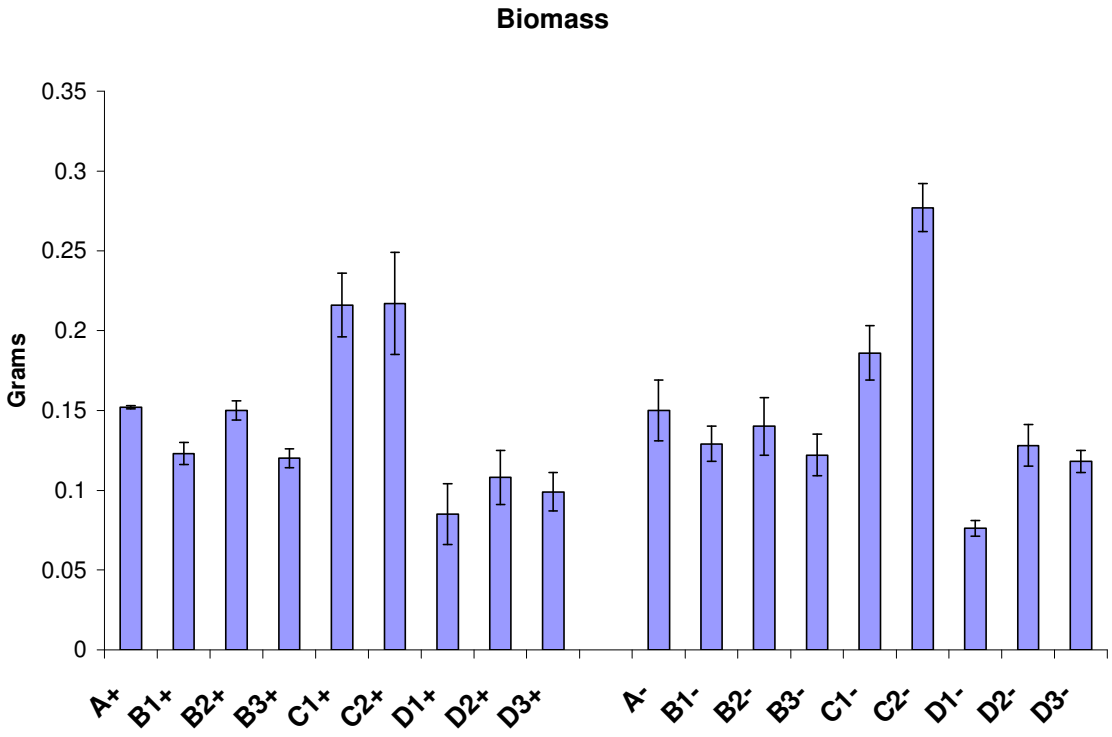

Fig. 20. Biomass of WT (Gv29-8) and mutants. Grown in VMS Fe+ and VMS Fe- liquid medium. Liquid media was inoculated with conidia. A=WT, B=ΔTvsidD (Mutants: 1=#4, 2=#46, 3=#75), C=ΔTvnps6 (Mutants: 1=#4, 2=#16), D=ΔΔTvsidDTvnps6 (Mutants: 1=#5, 2=#9, 3=#10). "+" and "-" signify VMS Fe+ and VMS Fe- media. Bars represent average weight in grams of three repetitions, and error bars show standard error.

To ascertain the importance of reductive iron assimilation (RIA), growth on agar in the presence of the chelator BPS was measured. Wild-type and a single strain of each mutant were grown on four types of agar: VMS Fe+, VMS Fe-, VMS Fe+ with BPS, and VMS Fe- with BPS. Inoculation was with conidia in the center of the plate and values for radial growth were determined at four days of incubation. The radial growth

measurements are shown in Figure 21. Strong inhibition was exerted by the chelator on both the ΔTvnps6 mutants and the double mutants under both BPS treatments compared to wild-type.

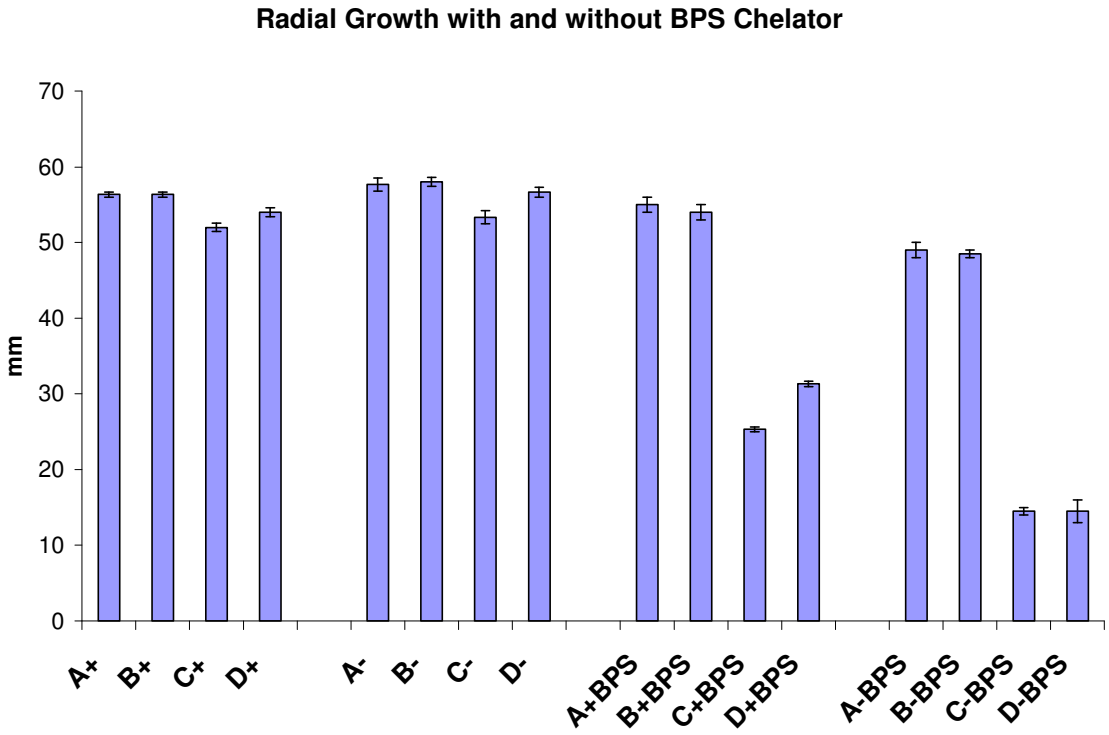

Fig. 21. Radial growth of wild-type (WT) and mutants with BPS chelator. Grown on Fe+, Fe-, Fe+ with BPS and Fe- with BPS agar medium. A=Wild-type, B=ΔTvsidD, C=ΔTvnps6, D=ΔΔTvsidDTvnps6. A single strain of each mutants (all transformant #4) were chosen. "+", "-", "+BPS", and "-BPS" denote Fe+, Fe-, Fe+ with BPS, and Fe- with BPS media. Values represent the average diameter in mm of three repetitions and error bars show standard error.

A subsequent experiment was performed in a liquid medium to confirm that ΔTvnps6 mutant growth is severely inhibited relative to wild-type. After four days of growth in Fe- media with 100μM BPS, wild-type biomass was significantly greater than both of the ΔTvnps6 mutants tested (Figure 22).

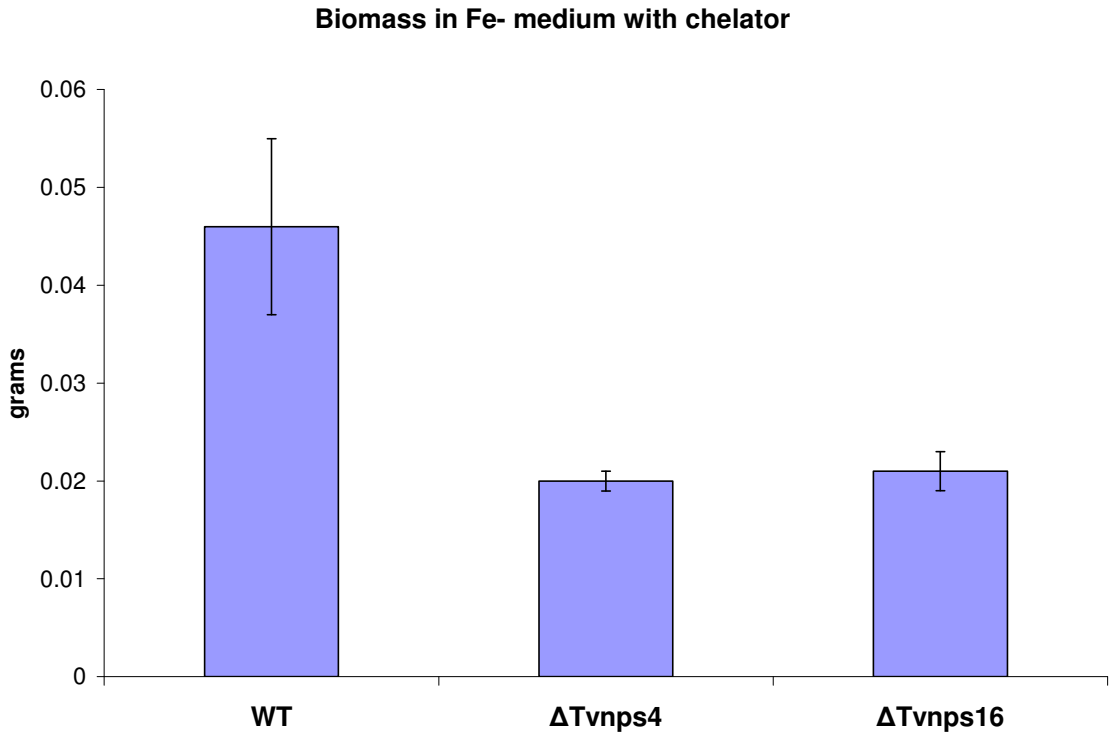

Fig. 22. Biomass growth of WT and ΔTvnps6 with BPS chelator. Biomass in Fe- media with 100μM of BPS. The average biomass of three repetitions is shown with standard error bars.

3.3.2. Conidiation and germination

The ability of the strains to produce conidia after four days incubation on VMS Fe+ and VMS Fe- agar is presented in Figure 23A, with values presented as the proportion relative to wild-type sporulation. On the Fe+ medium, conidia formation by the wild-type was significantly greater than all ΔTvsidD strains but significantly less than ΔTvnps4, ΔTvnps 16, and ΔΔTvsidDTvnps9. On the Fe- medium, wild-type conidiation was significantly greater than ΔTvsidD46, ΔTvsidD75, ΔΔTvsidDTvnps4 and ΔΔTvsidDTvnps5, whereas it was significantly less than ΔTvnps16.

As siderophore mutants in other studies have shown reductions in conidiation under oxidative stress (Schrettl et al., 2007), the effect of hydrogen peroxide on conidiation was evaluated with wild-type, and single strains of ΔTvsidD (ΔTvsidD4) and ΔTvnps6 (ΔTvnps4) mutants (Figure 23B). Conidiation of wild-type was significantly greater than the ΔTvnps6 mutant on Fe+ medium. On Fe- medium, wild-type was greater than ΔTvnps6 but less than ΔTvsidD. For the Fe+2mM hydrogen peroxide treatment, wild-type was less than ΔTvsidD. For both hydrogen peroxide treatments, wild-type was greater than ΔTvnps6. As for intrastrain variability, wild-type and mutants all showed reduced growth under the hydrogen peroxide treatments compared to Fe+, with the exception of WT Fe+ vs. WT Fe-2mM.

Germination on 2mM H_2O_2 as a proportion of germination without hydrogen peroxide is presented in Figure 24. Wild-type germination was significantly greater than ΔTvsidD46 and ΔΔTvsidDTvnps9, but significantly less than ΔTvsidD4, ΔTvnps4, and ΔΔTvsidDTvnps10.

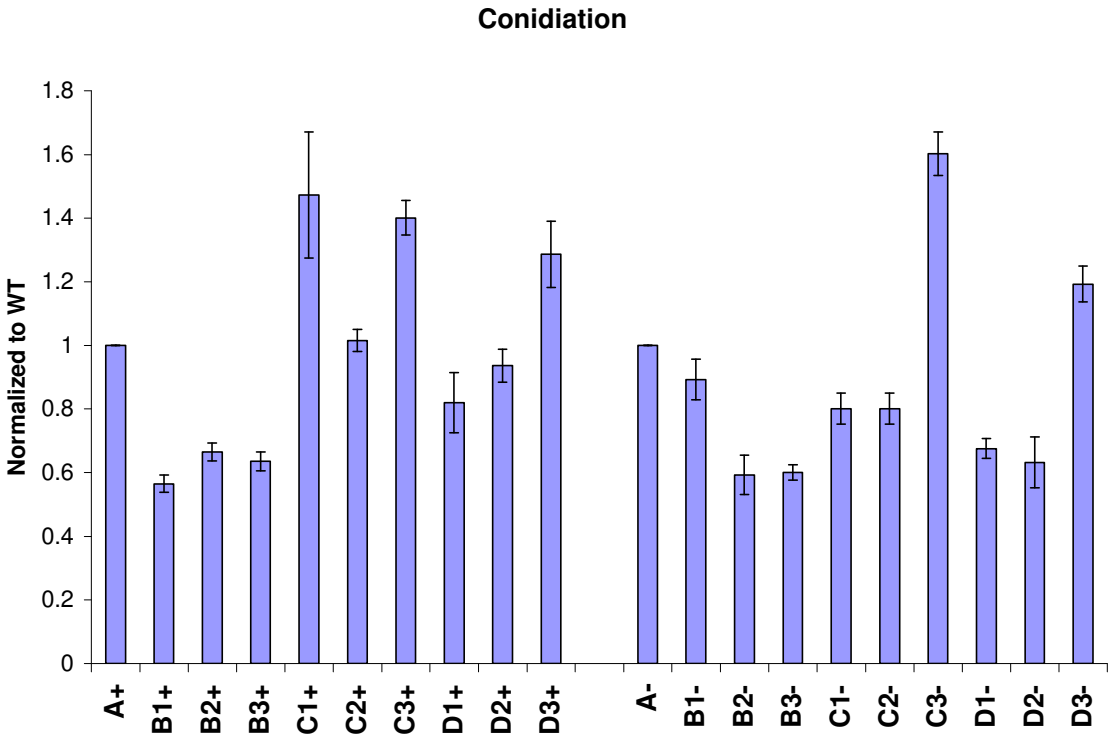

Fig. 23A. Conidiation of WT and mutants. Grown on Fe+ and Fe- medium. Conidiation of mutants is presented as a proportion of wild-type. Conidia were harvested and counted after 4 days incubation. A=Wild-type, B=ΔTvsidD (Mutants: 1=#4, 2=#46, 3=#75), C=ΔTvnps6 (Mutants:1=#4, 2=#15, 3=#16), D=ΔΔTvsidDTvnps6 (Mutants: 1=#4, 2=#5, 3=#9). "+" and "-"signify Fe+ and Fe- media. Error bars represent standard error.

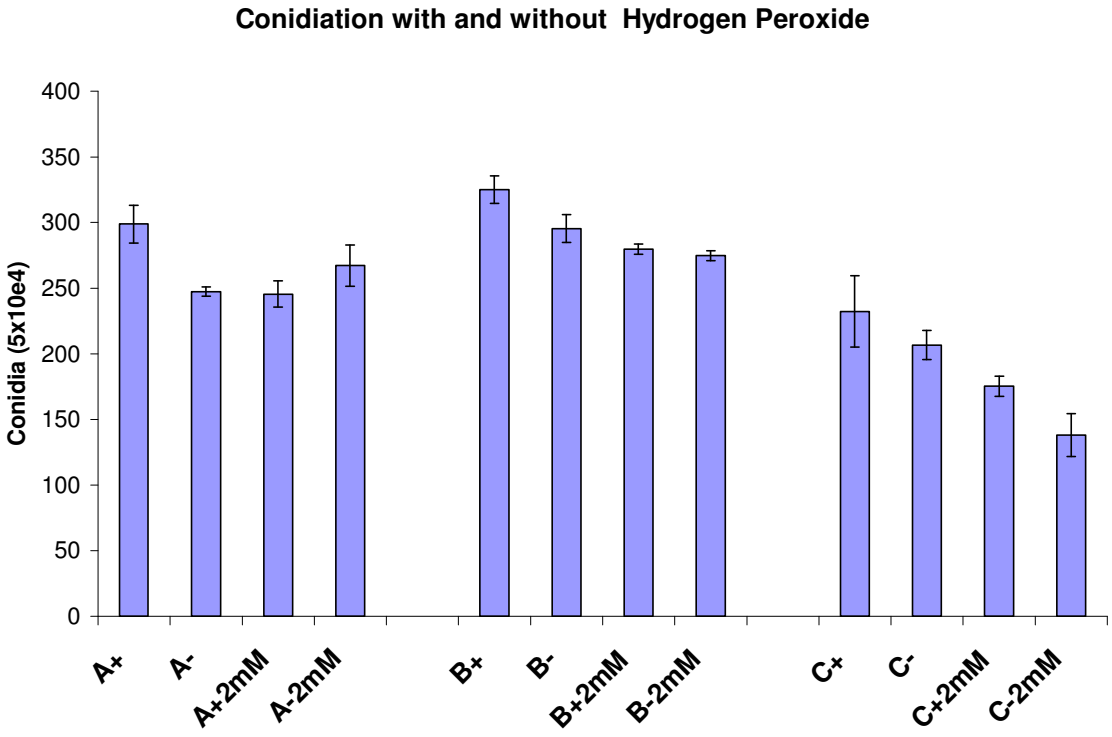

Fig. 23B. Conidiation of WT and mutants with H_2O_2 stress. Strains tested are A=Wild-type, B=ΔTvsidD mutant#4, C=ΔTvnps6 mutant#4. Conidiation was determined on VMS Fe+ (+), VMS Fe-(-), VMS Fe+ with 2mM H_2O_2 (+2mM), or VMS Fe- with 2mM H_2O_2 (-2mM). Conidia were harvested after 4 days incubation. Error bars represent standard error.

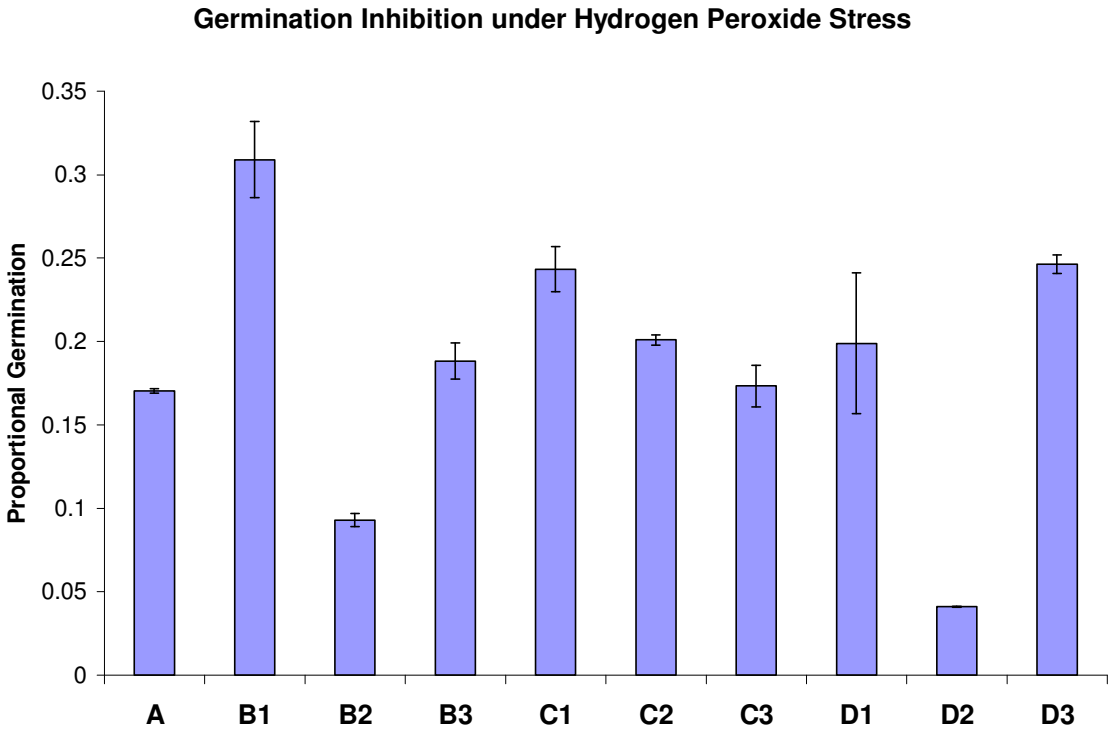

Fig. 24. Germination of WT and mutants with H_2O_2 stress. Grown on normal VMS medium with 2mM hydrogen peroxide. Germination is presented as a proportion of germination in absence of H_2O_2. A= wild-type, B=ΔTvnps6, C=ΔTvsidD, D=ΔΔTvsidDTvnps6. Error bars are standard errors.

3.3.3. Confrontation and biocontrol

All mutants performed identically to wild-type in the confrontation assay against *R. solani*. All strains overgrew the pathogen within eleven days regardless of the medium (Fe+ and Fe-). Typical confrontation plates are shown in Figure 25. Coiling of hyphae of strains of *T. virens* around the hyphae of *R. solani* was confirmed by microscopy, with mutants showing no loss of this mycoparasitic trait.

Similarly, there was no reduction of the biocontrol abilities in the mutants. All mutants prevented *P. ultimum* infection on cotton to the same degree as the wild-type strain. The biocontrol experiment is depicted in Figure 26, with the positive control containing *P. ultimum* but no *Trichoderma* strains, and the negative control containing neither *P.ultimum* nor *Trichoderma* strains. A grading scale of 3(dead), 2(diseased with visible lesions) and 1(healthy) was used with the average index presented in Figure 26.

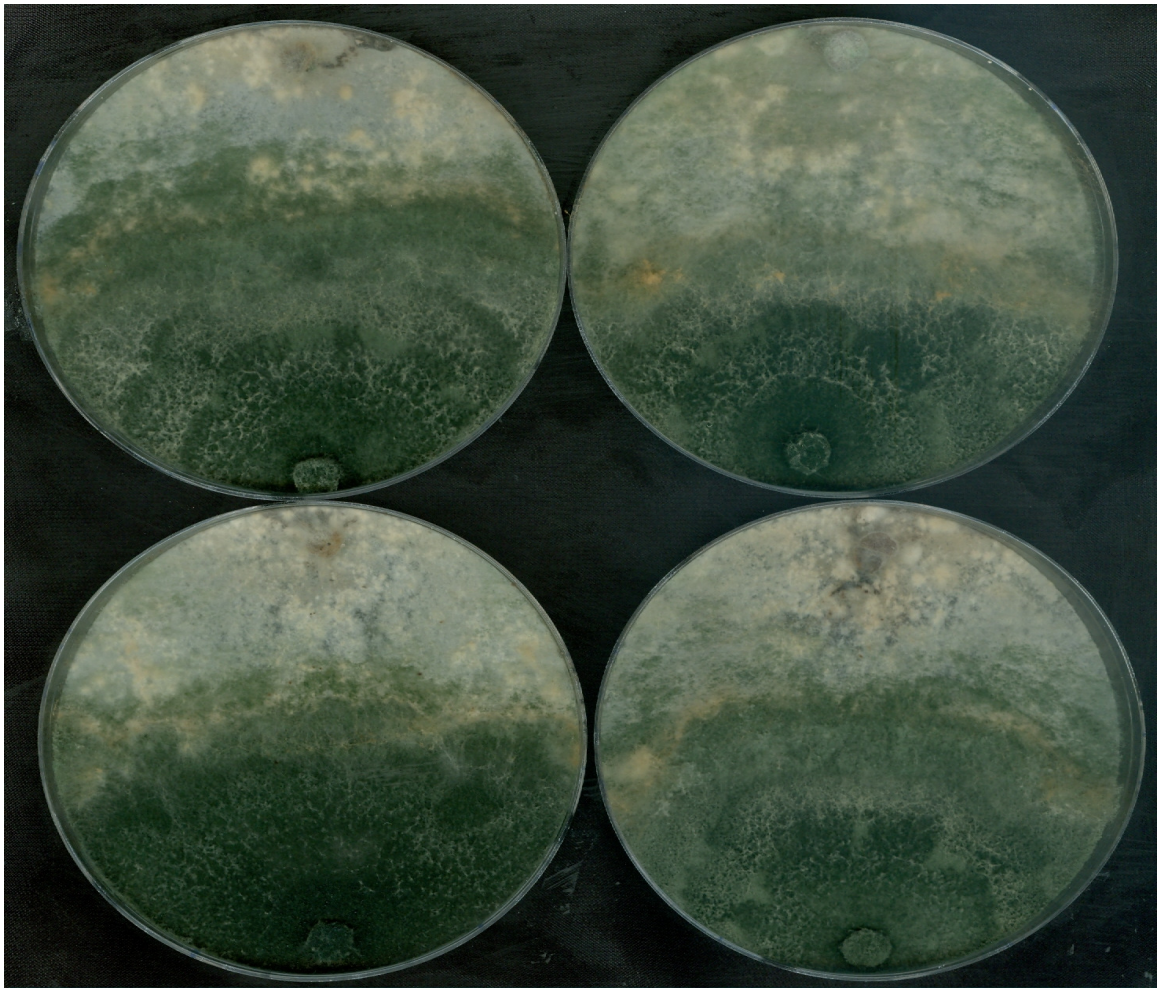

Fig. 25. Confrontation against *Rhizoctonia solani*. Grown on Fe- plates after 11 days of incubation. Clockwise from top left: wild-type, ΔTvsidD4, ΔΔTvsidDTvnps4, ΔTvnps4. The *Trichoderma* strains initiated in the lower half of the plate have overgrown the lighter-colored *P. ultimum* and reached the opposite edge of the plate.

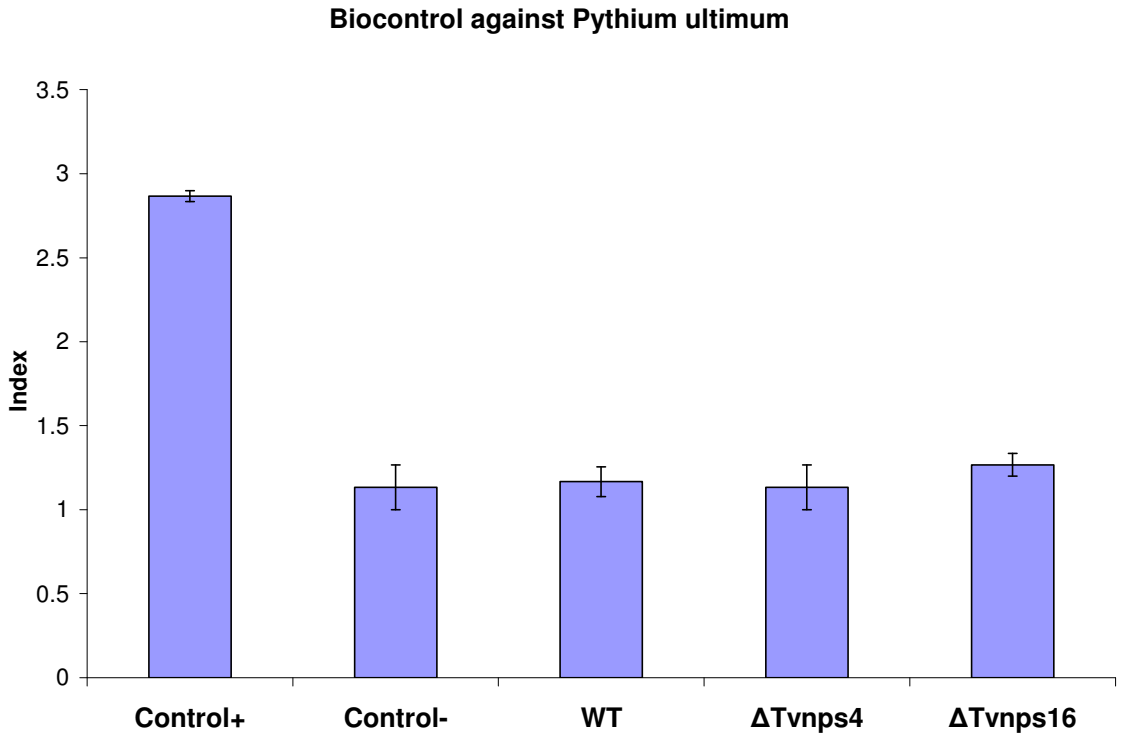

Fig. 26. Biocontrol against *Pythium ultimum*. Hosts were cotton seedlings. Grading scale was 3=dead, 2=diseased with visible lesions, 1=healthy, with the average index of ten repetitions presented. Error bars are standard errors. The positive control lacks *Trichoderma*, whereas the negative control lacks both *Trichoderma* and the pathogen *P. ultimum*.

3.3.4. Root colonization

Averages for the number of colonies/mm of maize root for two mutant and the wild-type strains are presented in Figure 27. There were no significant differences among the strains, wild-type, ΔTvsidD4 and ΔTvnps4 (when a single mutant of each

type was to be tested, the lowest number was chosen. In this case, for all three types of transformant, the mutant was #4).

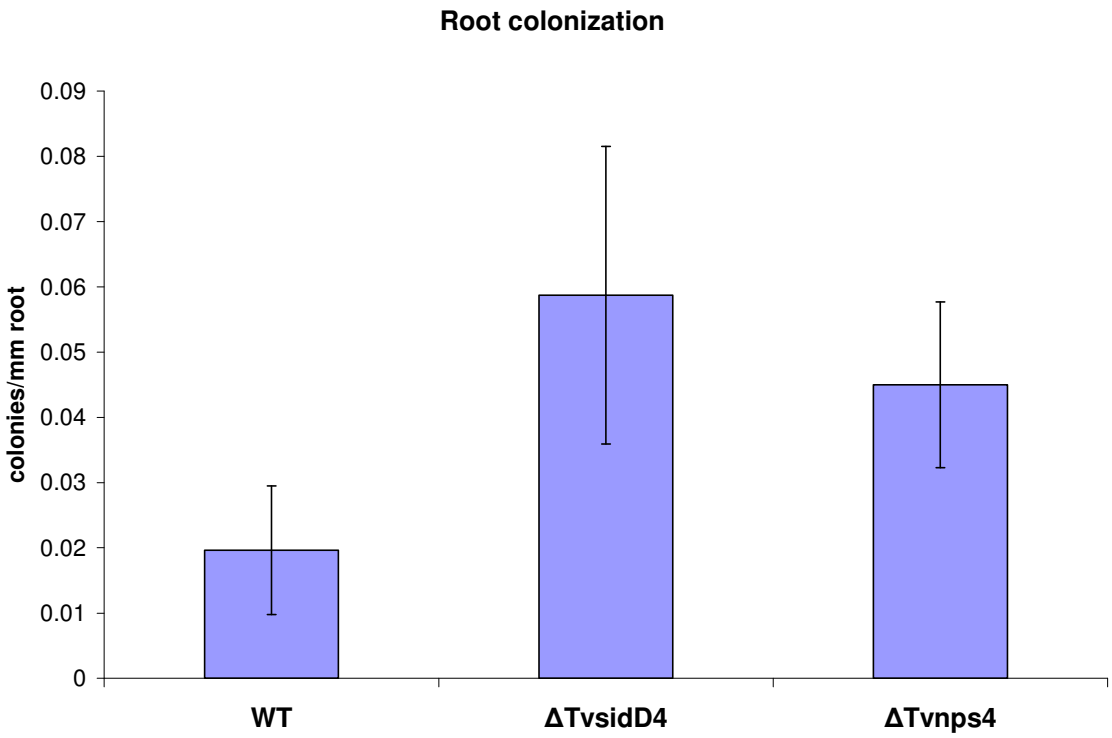

Fig. 27. Root colonization of WT and mutants on maize. Average number of colonies of wild-type (WT) and two mutants on the roots of *Zea mays* seedlings. The values are colonies per millimeter of root length with standard error bars.

3.3.5. Growth with chelators

In order to determine the relative contribution of RIA to *T. virens* growth, biomass of wild-type was measured in liquid media of varying iron-concentrations with and without the BPS chelator. Results are presented in Figure 28 and Table 5. Without the chelator, there were no significant differences in biomass production among the three iron treatments. However, with the chelator, biomass in Fe+10 with BPS was significantly greater than Fe- with BPS and Fe+1 with BPS. Growth under all three iron levels was significantly greater in the absence of BPS than in its presence.

Similarly, biomass production by wild-type was also tested with the membrane-permeable chelator 2,2'-dipyridyl (2DP) at a concentration of 100µM. The Fe- with 2DP was significantly less than the Fe- and Fe+1 treatments (Figure 29). No other differences were significant.

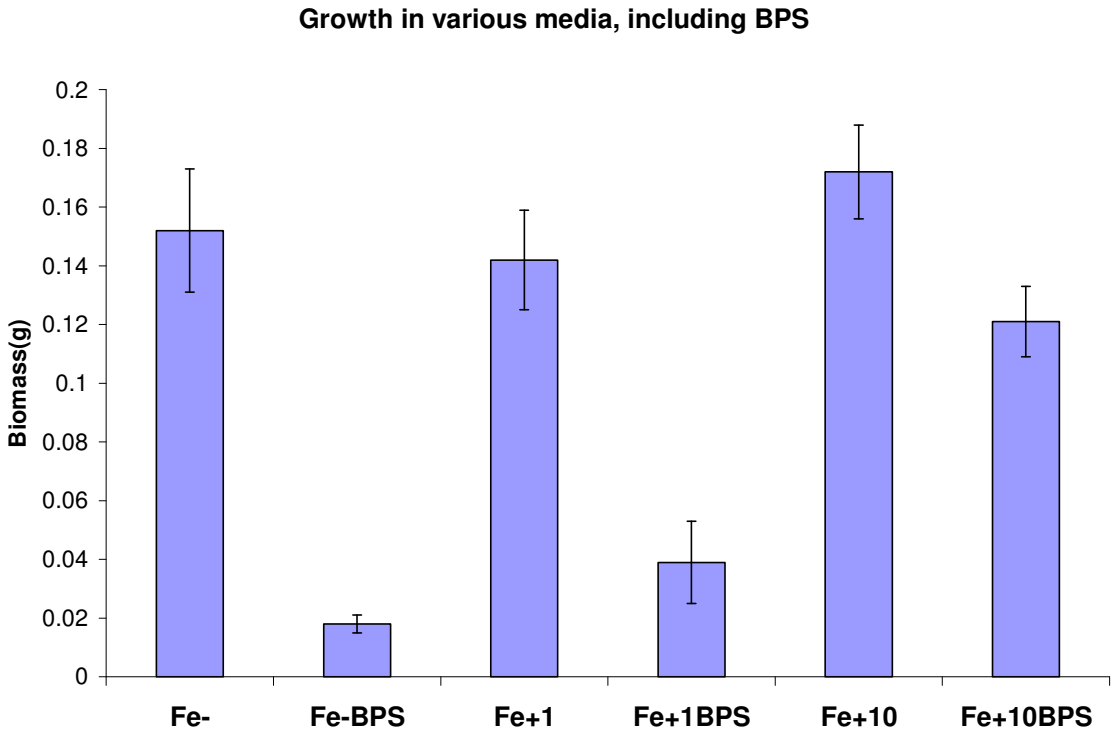

Fig. 28. Biomass of WT under various BPS treatments. Average biomass (dry weight) of wild-type after four days incubation in different media, with or without 100µM BPS. Media are, from left to right, VMS Fe-, VMS Fe- with BPS, VMS Fe+1µM $FeSO_4$, VMS Fe+1µM $FeSO_4$ with BPS, VMS Fe+10µM $FeSO_4$, VMS Fe+10µM $FeSO_4$ with BPS. Values represent the average of 3 repetitions with error bars corresponding to standard errors.

Table 5 Biomass (dry weight) of wild-type grown in various media with BPS. Analyzed with Fisher's Protected Least Significant Differences Test.

Comparison	Mean Difference	P-value	Significance
Fe-,Fe- with BPS	0.134	<0.0001	S
Fe-,Fe+1μM $FeSO_4$	0.010	0.6424	-
Fe-, Fe+10 μM $FeSO_4$	-0.019	0.3753	-
Fe- with BPS, Fe+1μM $FeSO_4$ with BPS	-0.021	0.3444	-
Fe- with BPS, Fe+10 μM $FeSO_4$ with BPS	-0.102	0.0004	S
Fe+1μM $FeSO_4$, Fe+1 μM $FeSO_4$ with BPS	0.103	0.0004	S
Fe+1 μM $FeSO_4$, Fe+10 μM $FeSO_4$	-0.029	0.1877	-
Fe+1 μM $FeSO_4$ with BPS, Fe+10 μM $FeSO_4$ with BPS	-0.082	0.0022	S
Fe+10 μM $FeSO_4$, Fe+10 μM $FeSO_4$ with BPS	0.051	0.0318	S

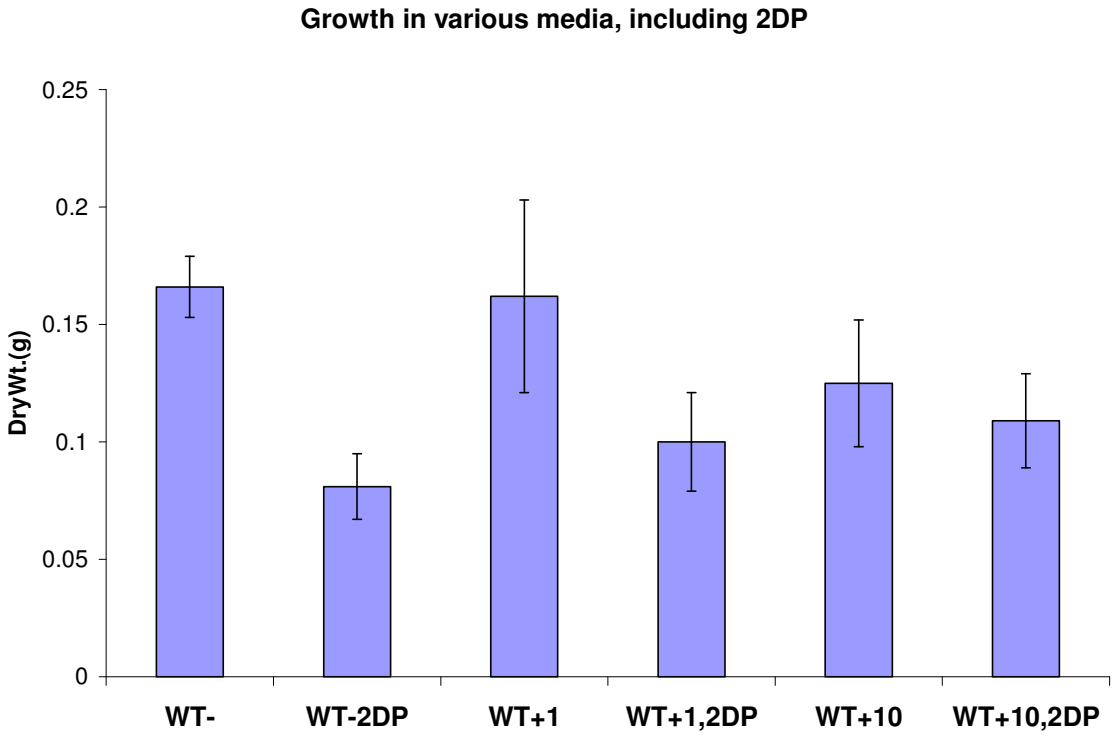

Fig. 29. Biomass of WT under various 2DP treatments. Biomass (dry weight) of wild-type (WT) after four days incubation in different media, with or without 100µM 2DP. Media are, from left to right, VMS Fe-, VMS Fe- with 2DP, VMS Fe+1µM $FeSO_4$, VMS Fe+1µM $FeSO_4$ with 2DP, VMS Fe+10µM $FeSO_4$, VMS Fe+10µM $FeSO_4$ with 2DP. Values are the average dry weight of three repetitions with error bars corresponding to standard errors.

4. DISCUSSION

4.1. HPLC analyses

HPLC analyses were performed at 435nm to detect hydroxamate siderophores. Analysis of the wild-type (Gv 29-8) with (Fe+) and without (Fe-) iron showed a prominent peak at 12.7 minutes under iron-depleted conditions (Figure 6). Lack of a peak under iron-replete conditions (~10µM Fe) demonstrates that transcription of genes encoding siderophore-producing NRPSs is repressed in iron-replete media. Concentrations of iron exceeding 10µM have generally been regarded to repress siderophore biosynthesis in most microorganisms (Leong and An, 1997), so our result is expected and our media sufficiently iron-depleted or iron-replete. Based on siderophore standards, the peak represents the biosynthesis of a coprogen-type siderophore by *T. virens*. This is similar to the production of coprogen in *Cochliobolus heterostrophus* (Lee et al., 2005), *Neurospora crassa*, and *Alternaria brassicicola* (Oide et al., 2006), and *Magnaporthe grisea* (Hof et al., 2009). These fungi contain an NRPS with homology to *TvNPS6*. In addition, coprogen and coprogen B have been detected in several *Trichoderma* strains (Anke et al., 1991). For the studies presented in this thesis, all subsequent filtrates submitted for HPLC analysis were from growth in the iron-depleted medium.

The mutant ΔTvsidD grown under iron-depleted conditions showed an identical chromatogram to the wild-type (Figure 7). Disruption of the *TvSIDD* gene had no

apparent effect on the production of the putative siderophore. As the *TvSIDD* gene is homologous to genes encoding fusarinine-producing NRPSs in *Aspergillus fumigatus* (Schrettl et al., 2007), this chromatogram suggests that the hydroxamate detected is not a fusarinine-type siderophore. In contrast, neither the ΔTvnps6 strain nor the double mutant showed the siderophore peak at 12.7 minutes (Figures 8 and 9). Evidently, disruption of *TvNPS6* prevents the production of a coprogen-type siderophore.

As the role of the NRPS TvSidD was not clear, the intracellular extracts of wild-type and ΔTvsidD were compared. This would reveal whether the TvSidD product was an intracellular siderophore. In Figure 10, it is shown that the ΔTvsidD strain retains the peak of the putative intracellular siderophore ferricrocin (of the ferrichrome family) at 10.9 minutes. Thus, the identity of the *TvSIDD* gene product was not resolved by our HPLC analysis.

4.2. Detection and confirmation of disruptions

With 44% of the transformants successfully growing and reproducing through serial passages on medium containing hygromycin, and three of the first 18 mutants tested showing a disruption in the target gene (Figures 11 and 12), the single crossover technique was an effective means of generating mutants. Several *TvNPS6* mutants (ΔTvnps4, ΔTvnps15, ΔTvnps16) were demonstrated to be generated by this approach (Figure 13). PCR amplification of a unique fragment in a second set of transformants verified double mutants ΔΔTvsidDTvnps4 , ΔΔTvsidDTvnps5, ΔΔTvsidDTvnps9, and

ΔΔTvsidDTvnps10 (Figure 15). Southern blots confirmed that there was homologous recombination for ΔTvnps4, ΔTvnps15, ΔTvnps16, ΔΔTvsidDTvnps4, ΔΔTvsidDTvnps5, ΔΔTvsidDTvnps9, and ΔΔTvsidDTvnps10 (Figures 17 and 18). Thus, mutants were generated for the two genes encoding NRPSs potentially involved in siderophore production in *T. virens*.

4.3. Phenotypic experiments

4.3.1 Growth

For area of mycelial growth, wild-type was significantly less than all mutants except for *ΔΔTvsidDTvnps9* for both Fe+ and Fe- treatments (Figure 19). This is unexpected as similar experiments (Schrettl et al., 2007; Hof et al., 2009) showed significant reductions in radial growth when a siderophore-producing NRPS is disrupted. The results are also at odds with the HPLC data presented; if the ΔTvnps6 and double mutants produce no siderophores, they would be expected to show reduced growth under iron-depleted conditions. Furthermore, after months of working with the mutants, no remarkable differences in growth appeared during plating or transfers. An argument could be made that area of mycelial growth is not an ideal measure since deficiencies in other phenotypic characteristics such as conidiation may allow greater allocation of energy for growth.

Growing the fungi in liquid media and then determining biomass as dry weight seemed preferable. Nevertheless, the data presented in Figure 20 show that the ΔTvnps6 strains outgrow the wild-type in both treatments, while double mutants #5 and #10 produce less biomass than wild-type in both treatments. Here, the ΔTvsidD mutants were not significantly different than wild-type.

From these first two bioassays, it seems that siderophore production, although clearly occurring in low-iron conditions, is not essential for growth of the fungus. Therefore, the effects of RIA on the mutants were investigated.

Figure 21 shows the results of growing wild-type and one strain of each mutant on four different agar media: VMS Fe+ (sufficient iron), VMS Fe- (low-iron, fungi employ siderophores and/or RIA), VMS Fe+ and BPS (Iron present, but chelation of ferrous iron by BPS, so RIA hindered), and VMS Fe- and BPS (low-iron, so BPS effect on RIA even more significant). Here the mutants incapable of producing a coprogen siderophore (ΔTvnps6, ΔΔTvsidDTvnps6) show growth less than or approximately equal to wild-type and ΔTvsidD on the Fe+ and Fe- media, contradicting the experiments (and supporting the empirical observations) discussed above. The addition of the chelator BPS significantly reduces the growth of ΔTvnps6 and ΔΔTvsidDTvnps6 mutants under both BPS treatments. On Fe- with BPS, these mutants show a greater degree of inhibition than on the Fe+ with BPS treatment, suggesting that the Fe+ with BPS treatment still has sufficient uncomplexed iron for the siderophore mutants to grow moderately using the RIA pathway. Studies with *A. fumigatus* (Schrettl et al., 2007) demonstrated similar results in which growth inhibition of siderophore mutants showed a

clear relationship to both iron and BPS concentrations. Wild-type and ΔTvsidD strains showed moderate growth reductions in Fe- with BPS compared to Fe-. ΔTvsidD's normal growth and the double mutants' phenotypic similarity to the ΔTvnps6 mutants suggest greater importance of the *TvNPS6* gene. It is almost certain that increasing BPS concentrations from our 100μM protocol would further reduce growth of all the strains, most drastically on those lacking a functional *TvNPS6* gene.

Liquid growth in Fe- media with BPS added was conducted on wild-type and two *TvNPS6* mutants. Corroborating the BPS experiment on agar, the ΔTvnps6 strains were significantly reduced compared to wild-type (Figure 22).

Thus, compared to wild-type, growth of the siderophore mutants (transformants disrupted in *TvNPS6*) showed pronounced inhibition under BPS treatments. This is expected as BPS blocks RIA by intercepting ferrous iron before it can reach the transmembrane Fet3/Ftr1 complex for oxidation and uptake. Without ferric-chelating siderophores to compensate for the loss of RIA, the siderophore mutants show reduced growth. No differences can be asserted confidently for the mutants under the Fe+ and Fe- treatments lacking BPS. The growth experiments suggest that RIA is more important for growth than siderophores since the siderophore mutants do as well or better under Fe- (RIA, no siderophores) than wild-type and ΔTvsidD do under Fe-BPS (siderophores, reduced RIA).

4.3.2 Conidiation and germination

Conidia production for all strains is presented in Figure 23A. Despite the similarity between wild-type and ΔTvsidD strains revealed by the HPLC analyses (i.e. siderophore production) and suggested by the growth data, the ΔTvsidD strains showed lower conidiation on both Fe+ and Fe- media. Compared to wild-type, the ΔTvnps6 strains showed a trend of greater sporulation on the Fe+ plates, but lower conidiation rates (except for the ΔTvnps16 strain) on Fe- media. The double mutants showed a similar trend, with slightly less sporulation in low-iron media.

Hydrogen peroxide's (2mM) effects on conidiation were determined with wild-type and the ΔTvsidD4 and ΔTvnps4 strains (Figure 23B). The siderophore mutant ΔTvnps4 conidiated significantly less than both wild-type and ΔTvsidD4 for all four treatments. Though neither wild-type nor ΔTvsidD4 showed strong negative effects from hydrogen peroxide, the siderophore mutant conidiated significantly less on the H_2O_2 plates compared to the Fe+ and Fe- plates. Given the contradictory data between Figures 23A and 23B, no conclusions can be made from these assays. Nevertheless, the reduced conidiation by the siderophore mutant ΔTvnps4 in the presence of H_2O_2 could be further investigated. Although the growth data suggest that RIA allows siderophore mutants to grow normally under low-iron conditions, the addition of H_2O_2 may increase iron demand for the synthesis of catalases and peroxidases to detoxify the reactive oxygen species to a degree beyond that which RIA can supply. Over the course of this project, the general trend has been that H_2O_2 in low-iron hindered *Trichoderma* more than in

iron-replete media. In other words, the deleterious effects of the Fenton Reaction are evidently less significant than the need for obtaining sufficient iron to synthesize the detoxifying enzymes.

Germination inhibition under H_2O_2 stress likewise failed to show any strong trends (Figure 24). Others (Schrettl et al., 2007) have discovered that conidia can carry their own reserves of iron stored in the conidial storage siderophore hydroxyferricrocin. Perhaps this iron reserve allows normal germination in the siderophore mutants (these mutants still have the intracellular siderophore ferricrocin), but this is soon depleted and subsequent development is hindered as the increased iron demand under oxidative stress cannot be met. Harvesting spores from H_2O_2 -treated plates then determining germination may be more informative as conidia produced by the ΔTvnps6 and double mutant strain under these conditions may have hydroxyferricrocin levels sufficiently low to affect germination.

Overall, the results from the conidiation and germination studies do not show any consistent trends in the absence of hydrogen peroxide. Studies with *Magnaporthe grisea* Δnps6 mutants showed reduced growth, conidiation and heightened sensitivity to hydrogen peroxide (Hof et al., 2009). They also recorded reduced catalase activity in the siderophore (coprogen) mutants. Much higher concentrations of H_2O_2 (2-20mM) were used and these experiments followed a day-night rhythm that also could have affected the phenotype. In the studies with *M. grisea* and *A. fumigatus*, greater time was allowed for sporulation than in the experiments with *T. virens* (Hof et al., 2009; Schrettl et al., 2007). Thus, higher concentrations of H_2O_2 and/or longer experiments may reveal

inhibition of the ΔTvnps6 and double mutant strains. Finally, given the large intrastrain variability, new protocols could be developed to obtain more consistent results. In summary, the results suggest that while extracellular siderophores may play a role in germination and conidiation, intracellular siderophores are more important, particularly under oxidative stress.

4.3.3. Confrontation, biocontrol and root colonization

All three mutants tested performed identically to wild-type in confrontation with *R. solani*, so low-iron did not compromise the antifungal capability of the mutants (Figure 25). No obvious visual differences between wild-type and the mutants were observed.

Likewise, the biocontrol assay showed no loss of effectiveness in the mutants to protect cotton seedlings against *P. ultimum* (Figure 26). It is notable that *T. virens* has been found to control oomycetes like *Pythium* and *Phytophthora* through production of gliovirin (Howell et al., 1993), which utilizes the same diketopiperazine building block as the coprogen siderophores (Figure 1). Nevertheless, research has also shown that *T. virens* mutants deficient in both mycoparasitism and antibiotic production still inhibited *R.solani* by inducing the cotton host to generate terpenoid aldehydes and increase peroxidase activity in the roots (Howell, 2004). *Trichoderma* was proposed to prevent *Pythium* infection of cotton by preventing susceptible germinating seeds from releasing compounds stimulatory to the latent pathogen (Howell, 2004). By this mechanism, the

biocontrol agent consumed sufficient germinating seed exudates to prevent pathogen activation.

Finally, the root colonization results did not show significant differences among the strains assayed (Figure 27). As only putative siderophore genes were disrupted and the media is not iron depleted, this is not surprising. Another consideration is that these experiments were from sterile hydroponics systems rather than soil environments. The rationale for this assay was that the host may produce a defensive oxidative burst upon initial infection that may have affected the mutants. The mutant fungi are probably using their low-affinity pathway to obtain iron if it is not too scarce. If the plant, which has been in the MS medium two days longer than the fungi, has already begun to deplete the iron, all strains can utilize functional RIA systems. From the growth discussion above, it seems that this is the more common high-affinity pathway in *T.virens*.

In summary, there were no significant differences for any of these three bioassays. The versatility of *T. virens* as a biocontrol species mentioned above is significant and it seems in light of the growth data that RIA can supply sufficient iron. It could be argued that in a more complex environment with a full suite of microorganisms and more variability in abiotic parameters (nutrients, moisture, pH, etc.), iron competition will be more intense and siderophore production would be necessary. Moreover, a combination of very low bioavailability of iron combined with the oxidative burst of the host which can be elicited by *T. virens* (Djonović et al., 2006a) may pose problems for the siderophore mutants since hydrogen peroxide did show effects (Figure 23B).

4.3.4. Growth with chelators

The purpose of these assays was to ascertain the contribution of RIA in the growth of the wild-type strain before considering the mutants. The membrane-impermeable BPS showed that wild-type functions equally well in all three treatments lacking BPS, with its success at lower iron concentrations attributable to RIA and/or siderophores. By adding BPS to the media, RIA is impeded and the fungus relies increasingly on siderophores. From the results in Figure 28, it seems that siderophore production by the wild-type cannot compensate for the loss of RIA in Fe- with BPS and Fe+1µM with BPS treatments. In the Fe+10µM with BPS treatment, biomass is still reduced compared to the Fe+10µM treatment, but is significantly higher than the other BPS treatments with lower iron. The 100µM of chelator is evidently becoming saturated.

The membrane-permeable 2,2-dipyridyl chelator showed less inhibiting effects, although there did seem to be a (non-significant) trend of chelator saturation as iron concentrations increased (Figure 29). In the Fe- with 2DP media, there was significantly less biomass than the Fe- and Fe+1 treatments. Oddly, the Fe+10 treatment biomass was not significantly greater than any of the BPS treatments. The non-chelator treatments were not significantly different from each other.

The BPS data clearly supports the hypothesis that RIA is more important than siderophore production for *T. virens*. The 2DP data is not clear, especially since others have shown that 2DP is strongly inhibiting in *C. heterostrophus* (Oide et al., 2006).

However, Oide et al. used agar plates rather than liquid media and also added higher concentrations of 2DP.

The nature of the 2DP chelator is different from BPS in that 2DP binds ferrous iron in a 1:1 ratio and uses 2 nitrogen ligands. The ligands are the respective lone pairs of two nitrogen atoms in the same uncharged aromatic ring. In contrast, BPS is a much larger molecule and binds ferrous iron with two anionic oxygen ligands in a 3:1 BPS:metal ratio (Yokoyama et al., 1999). Thus the BPS-iron(II) complex has a charge of -4 (an individual uncomplexed BPS has a -2 charge and cannot enter the membrane). Although siderophores have some affinity for other trivalent cations (aluminum, gallium, indium) these elements are usually quite scarce, which is in marked contrast to the divalent cations, such as zinc, manganese and copper, which may be complexed by the BPS and 2DP. It has been observed that copper (II) was preferentially bound by ethylene diamine over iron(II) (i.e. higher stability constant) since copper prefers this chelator's nitrogenous ligands (Kosman, 1994) Moreover, the concentrations and availability of the divalent ions may vary on opposite sides of the membrane, with intracellular metals usually bound to ligands and much less accessible than the metal salts occurring in the extracellular environment (Kosman, 1994). In short, because of these variables, an explanation for the discrepancy between chelators cannot be offered with confidence.

5. CONCLUSIONS AND FUTURE DIRECTIONS

5.1 Conclusions

This project determined that *T. virens* has two genes putatively encoding extracellular siderophore-producing NRPSs, *TvSIDD* and *TVNPS6*, but only the latter generated a detectable siderophore product. Although many fungi produce different derivatives within a single hydroxamate family, *T. virens'* possession of two genes possibly producing fusarinines and coprogens is noteworthy. Anke (Anke et al., 1991) did observe that *T. pseudokoningii* and *T. longbrachiatum* produced both coprogens and fusarinines, though the other seven *Trichoderma* strains tested made only coprogens. Since siderophore production has metabolic costs, producing two separate siderophores through two different NRPSs could be considered redundant.

Coprogen production may have become selected for since the tri-ester fusarinines are more susceptible to hydrolysis by esterases, such as those produced by decaying plant cells and soil bacteria such as *Bacillus* and *Streptomyces* (Winkelmann, 2007). Coprogen also has an ester bond attaching the third trans-fusarinine to the diketopiperazine dimerum acid, though attaching an acetyl or methyl group to the N^2 atom of this third molecule can shield the ester (Renshaw et al., 2002) and also allow structural diversity (Haas et al., 2008). The methyl groups create a more lipophilic molecule, whereas hydroxyl groups attached to either end of the trihydroxamate make the molecule more hydrophilic (Renshaw et al., 2002). Additionally, if the ester bond is

cleaved, the remaining dimerum acid can still function as a siderophore, albeit a weaker tetradentate one. Coprogens are not as durable as hexapeptide ferrichrome-type siderophores, which predominate among saprophytes, but they are not as costly to produce.

Another observation was that, unless H_2O_2 was present, the siderophore mutants (ΔTvnps6, ΔΔTvsidDnps6) lacking a functional *TvNPS6* gene generally performed as well in iron-depleted media as the wild-type and were just as effective in biocontrol. This suggests RIA is the primary pathway for iron acquisition in *T. virens*. In contrast, loss of the extracellular siderophores fusarinine C (a.k.a.fusigen) and TAFC lowered growth rates and conidiation in *A. fumigatus* grown in Fe- media, whereas 150% greater application of the chelator BPS (250μM) did not alter growth of wild-type strains (Schrettl et al., 2007). Likewise, *M grisea* mutants defective in coprogen production showed lower growth rates and conidiation in Fe- media than wild-type (Hof et al., 2009). Perhaps *Trichoderma*'s existence as a saprophyte/symbiont puts it in a comparatively iron-rich soil environment that would provide more substrates for RIA, such as humic acids, fulvic acids, iron salts, etc.. Secretion of acidic compounds (e.g. caffeic acid) by plant roots would lower the pH of the microenvironment and solubilize more iron. Furthermore, hydroxamate siderophores' efficacy decreases with lower pH as protons increasingly compete for the ligands. MFS transporters are not particularly abundant in the *T. virens* gene clusters, implying that siderophore/xenosiderophore uptake is not as critical as in other saprophytes. In contrast, *M. grisea* and *A. fumigatus* inhabit more restricted niches as leaf and human pathogens with fewer opportunities for

RIA. Deletion of the RIA system's FtrA iron permease in *A. fumigatus* did not affect virulence, whereas loss of siderophores did (Schrettl et al., 2004). Although *A. fumigatus* also exists as a saprophyte, it encounters a very iron-depleted environment as a pathogen. Iron must be removed by TAFC from high-affinity complexes with transferrin. Although some microorganisms, such as *Candida albicans*, have specialized receptors for ferritin-type molecules, it is not especially common. Human transferrin has 679 amino acids, so it is likely more difficult to maneuver this molecule through the cell wall into position for RIA. Similarly, the *C. heterostrophus* host, rice, has iron bound by phytoferritins.

The indications we detected of siderophore mutant heightened sensitivity to H_2O_2 were corroborated by other studies (Oide et al., 2006: Schrettl et al., 2007: Hof et al., 2009). The Oide *et al.* study showed that the *C. heterostrophus Δnps6* mutants were inhibited at half the concentration of hydrogen peroxide as wild-type (8mM vs. 16mM), while the Hof *et al*. *M. grisea* research showed mutant inhibition at 16mM and wild-type inhibition at 20mM. The Schrettl *et al.* study matched our observation that all strains met challenges by H_2O_2 better in iron-replete media than in iron-depleted media. Both the *C. heterostrophus* and *M. grisea* studies showed strong inhibition exerted on the mutants by the superoxide generator KO_2.

Despite *TvSIDD*'s homology to genes encoding siderophore-producing NRPSs, disruption of this gene did not reduce the putative siderophore peak on the HPLC analysis, so it is unclear what this gene's role is. One possibility is that the TvNps6 NRPS produces sufficient siderophores, rendering the TvSidD peptide synthetase

superfluous and nonfunctional. The *TvSIDD* gene cluster depicted in Table 1 show *T. virens* missing several genes present in the *A. fumigatus* cluster, so it is possible that key enzymes are missing and/or a defective protein is produced that was not detected by HPLC. Alternatively, considering iron deficiency derepresses genes encoding siderophore-producing NRPSs, perhaps the transcription of *TvSIDD* is delayed relative to that of *TvNPS6* and the RIA genes and incoming iron from these pathways keep the *TvSIDD* locus unexpressed.

Another more conjectural possibility is that in the absence of selection pressure, the "redundant" NRPS has evolved/been modified to serve another purpose. Research has shown that *Trichoderma* spp. can withstand fairly high levels of heavy metals (Kredics et al., 2001a; Kredics et al., 2001b) and can degrade toxicants such as (metallo)cyanide, arsenic, polyphenols, and hydrocarbons (Harman et al, 2004). In addition, the hydroxamate siderophores of the bacteria *Rhizobium* and *Bacillus* have been observed to chelate toxic Al^{3+} (Rogers et al., 2001; Hu and Boyer, 1996), which damages plant roots. Like *Trichoderma*, *Rhizobium* is a plant symbiont. Hydroxamates are stable down to a pH of 2.0 (Winkelmann, 2001) and trivalent aluminum becomes mobile at pH 4.7 (aluminum hydroxides in soils serve as buffers, reacting with protons to form Al^{3+} and water) (Schlesinger, 1997), so chelation by fungal hydroxamates could ameliorate damage to the plant. In a low-iron environment high concentrations of aluminum were observed to further increase siderophore production, though in iron-replete cultures the added aluminum did not elicit siderophore production (Hu et al., 1996). Aluminum

complexed to the siderophore vicibactin did not show any toxic effects towards *Rhizobium* (Rogers et al., 2001).

The most plausible new role for the redundant siderophore could be in copper metabolism. It was shown that the *S. cerevisiae* copper chaperone and transporter (Atx1p and Ccc2p, respectively) were expressed in response to iron depletion, not copper depletion (Philpott, 2006). Given *T. virens* apparent reliance on RIA and the requirement for RIA's Fet3 oxidase to be loaded with four copper atoms, ensuring an adequate supply copper is critical. On the other hand, studies of *T. viride* observed that the fungus was able to withstand high concentrations of copper by binding it to the cell wall (Anand et al., 2005). This calls to mind the Fit (facilitator of iron transport) proteins that bind siderophore-iron complexes to the cell wall of *S. cerevisiae* before the complexes are processed by the RIA system. Both iron and copper share the first RIA step of reduction by the Fre1p metalloreductase (Philpott, 2006). Of the divalent cations (including Fe^{2+}), only Cu(II) forms strong complexes with hydroxamates. Chelation of excess copper could prevent swamping of the low-affinity divalent transporter that would not only lead to Cu toxicity, but also preclude then entry of other essential divalent ions. Nevertheless, copper-hydroxamate chelates have a much different structure than those of iron (Van der Helm and Winkelmann, 1994), so this alternative role for TvSidD, like the others, is highly speculative.

In summary, this study suggests that RIA is the primary mechanism of iron uptake as siderophore mutants were not inhibited in the absence of an added chelator. Although

T. virens has two genes putatively encoding extracellular siderophore-producing NRPSs, only the TvNPS6 gene has a detectable product, which is a coprogen-type siderophore.

5.2 Future directions

In the immediate future, it will be informative to treat the mutants with larger quantities of hydrogen peroxide to see greater effects. Also, as the mutants are entirely dependent on RIA, perhaps increasing doses of the 2DP chelator, which may preferentially bind copper over iron, could reduce RIA by limiting copper. The logic would be that the wild-type would shift to getting more iron via siderophores, an option unavailable to siderophore mutants. This would require a media depleted in both iron and copper. In addition, adding the superoxide generator KO_2 to the media could possibly produce strong effects since superoxide can reduce ferric iron to ferrous iron and also generate hydrogen peroxide. In other words, KO_2 could supply both reactants of the Fenton Reaction (Howard, 1999; Madigan and Martinko, 2006)

Our lab has disrupted the "master siderophore gene", *TvSIDA*, which encodes the L-ornithine N^5-monoxygenase, the initial step of siderophore synthesis (Figure 2). Other studies examining these type mutants have seen large effects (Schrettl et al., 2007; Hof et al., 2009). Blocking the initial step leaves the fungus entirely dependent on RIA and the speculation above about copper (both dearth and excess) could be tested (in this condition, aluminum would almost certainly be toxic).

Conversely, the RIA system could be examined, annotated and mutated to see whether siderophores can offset the loss of RIA. The best target for mutation would be the genes encoding the Ftr1-Fet3 complex since it is specific for iron, whereas the metalloreductase homologous to *S. cerevisiae's* Fre1 may also have copper(II) as a substrate (see Introduction, p.4). In this altered state, it would be interesting to see whether *TvSIDD* makes a product if the coprogen siderophores cannot compensate sufficiently. Also, since iron is acquired by either taking in the entire Fe-siderophore complex through the Arn transporters or removing the iron from the siderophore by reducing it at the membrane (RIA), disrupting RIA may help determine which transporters are present. In these RIA mutants, ferrated (loaded) siderophores from other families (ferrichromes, fusarinines, catecholates) could also be added to see whether they can be utilized. Uptake of coprogen and possibly fusarinine would be predicted for *T. virens*.

REFERENCES

Alabouvette, C., Olivain, C., Steinberg, C., 2006. Biological control of plant diseases: The European situation. European Journal of Plant Pathology 114, 329-341.

Anand, P., Isar, J., Saran, S., Saxena, R.K., 2006. Bioaccumulation of copper by *Trichoderma viride*. Bioresource Technology 97, 1018-1025.

Anke, H., Kinn, J., Bergquist, K.E., Sterner, O., 1991. Production of siderophores by strains of the genus Trichoderma. Biometals 4, 176-180.

Ayers,W.A.,Lumsden,R.D., 1975. Factors affecting production and germination of oospores of three *Pythium* species. Phytopathology 65, 1094-1100.

Baek, J.M., Kenerley, C.M., 1998. The *ARG2* gene of *Trichoderma virens*: Cloning and development of a homologous transformation system. Fungal Genetics and Biology 23, 34-44.

Benitez, T., Rinco, A.M., Limon, M.C., Codon, A.C., 2004. Biocontrol mechanisms of *Trichoderma* strains. International Microbiology 7, 249-260.

Butt, T.M., Jackson, C., Magan, N., 2001. Fungi as Biocontrol Agents: Progress, Problems, and Potential, CABI International, London, U.K.

Chaverri, P., Samuels, G.J.,Stewart, E.L., 2001. *Hypocrea virens* sp. Nov., the teleomorph of *Trichoderma virens*. Mycologia 93:1113-1124.

Chet, I., Baker, R., 1981. Isolation and biocontrol potential of *Trichoderma harmatum* from soil naturally suppressive to *Rhizoctonia solani*. Phytopathology 71, 286-290.

Dix, D.R., Bridgham, J.T., Broderius, M.A., Byersdorfer, C.A., Eide, D.J., 1994. The *FET4* gene encodes the low-affinity Fe(II) transport protein of *Saccharomyces cerevisiae*. Journal of Biological Chemistry 269, 26092-26099.

Djonović, S., Pozo, M.J., Dangott, L.J., Howell, C.R., Kenerley, C.M., 2006a. Sm1, a proteinaceous elicitor secreted by the biocontrol fungus *Trichoderma virens* induces plant defense responses and systemic resistance. Molecular Plant-Microbe Interactions 19, 838-853.

Djonović, S., Pozo, M.J., Kenerley, C.M., 2006b. Tvbgn3, a β-1,6-Glucanase from the biocontrol fungus *Trichoderma virens*, is involved in mycoparasitism and control of *Pythium ultimum*. Applied and Environmental Microbiology 72, 7661-7670.

Djonović, S., Vargas, W.A., Kolomiets, M.V., Horndeski, M., Wiest, A., Kenerley, C.M., 2007. A proteinaceous elicitor Sm1 from the beneficial fungus *Trichoderma virens* is required for induced systemic resistance in maize. Plant Physiology 145,. 875-889

Eisendle, M., Oberegger, H., Zadra, I., Haas, H., 2003. The siderophore system is essential for viability of *Aspergillus nidulans*: Functional analysis of two genes encoding L-ornithine N^5-monooxygenase (*sidA*) and a nonribosomal peptide synthetase (*sidC*). Mol. Microbiol 49, 359-375.

Finking, R., Marahiel, M.A., 2004. Biosynthesis of nonribosomal peptides. Annu. Rev. Microbiol. 58, 453-488.

Foster L.A., 2002 Utilization and cell-surface binding of hemin by *Histoplasma capsulatum*. Canadian Journal of Microbiology. 48,437-442.

Fravel, D.R., 2008. Commercialization and implementation of biocontrol. Annu. Rev. Phytopathol. 43, 337-359.

Ghisalberti, E.L., Sivasithamparam, K., 1991. Antifungal antibiotics produced by *Trichoderma* spp. Soil Biol Biochem 23, 1011–1020.

Greenwood, N.N., Earnshaw, A., 1997. Chemistry of the Elements (2nd ed.), Butterworth-Heinemann, Oxford

Haas, H., 2003. Molecular genetics of fungal siderophore biosynthesis and uptake: The role of siderophores in iron uptake and storage. Applied Microbiological Biotechnology 62, 316-330.

Haas, H., Eisendle, M., Turgeon, B.G., 2008. Siderophores and fungal physiology and virulence. Annu. Rev. Phytopathol. 46, 149-187.

Halliwell, B., Gutteridge, J.M., 1984. Oxygen toxicity, oxygen radicals, transition metals and disease. Biochemistry Journal 219, 1-14.

Harman, G.E., Lorito, M., Lynch J.M. 2004. Uses of *Trichoderma* spp. to alleviate or remediate soil and water pollution. Advances in Applied Microbiology 56, 313-330.

Hassett, R., Dix, D.R., Eide, D.J., Kosman, D.J., 2000. The Fe(II) permease Fet4p functions as a low-affinity copper transporter and supports normal copper trafficking in *Saccharomyces cerevisiae*. Biochem. J. 351, 477-484.

Hof, C., Eisfeld, K., Antelo, L., Foster, A.J., Anke, H., 2009. Siderophore synthesis in *Magnaporthe grisea* is essential for vegetative growth, conidiation, and resistance to oxidative stress. Fungal Genetics and Biology 46, 321-332.

Howard, D.H., 1999. Acquisition, transport and storage of iron by pathogenic fungi. Clinical Microbiology Reviews 12, 394-404.

Howell, C.R., Stipanovic, R.D., 1983. Gliovirin, a new antibiotic from *Gliocladium virens*, and its role in the biological control of *Pythium ultimum*. Canadian Journal of Microbiology 29, 321-324.

Howell, C. R., Stipanovic, R. D. 1984. Phytotoxicity to crop plants and herbicidal effects on weeds of viridiol produced by *Gliocladium virens.* Phytopathology 74**,** 1346–1349

Howell, C.R., Stipanovic, R.D., Lumsden, R.D., 1993. Antibiotic production by strains of *Gliocladium virens* and its relation to the biocontrol of cotton seedling diseases. Biocontrol Science and Technology 3, 435-441.

Howell, C.R., 2003. Mechanisms employed by *Trichoderma* species in the biological control of plant diseases: The history and evolution of current concepts. Plant Disease 87, 4-10.

Howell, C.R., 2004. Understanding the mechanisms employed by *Trichoderma virens* to effect biological control of cotton diseases. Phytopathology 96, 178-180.

Hu, X., Boyer, G.L., 1996. Siderophore-mediated aluminum uptake by *Bacillus megaterium* ATCC 19213. Applied and Environmental Microbiology 62, 4044-4048.

Hwang, L., Mayfield, J.A., Rine, J., Sil, A., 2008. *Histoplasma* requires *SID1*, a member of an iron-regulated siderophore gene cluster, for host colonization. PLoS Pathogens 4, 1-9.

Jeger, M.L., Jeffries,P., Elad,Y., Xu, X.M., 2009. A generic theoretical model for biological control of foliar plant diseases. Journal of Theoretical Biology 256, 201-214.

Jones, J.D., Dangl ,J.L., 2006. The plant immune system. Nature 444, 323-329.

Jones, R. W., Lanini, W. T., Hancock, J. G., 1988. Plant growth response to the phytotoxin viridiol produced by the fungus *Gliocladium virens.* Weed Science. 36**,** 683–687.

Kosman, D.J., 1994. Transition metal ion uptake in yeasts and filamentous fungi. In:Winkelmann, G.,Winge, D.R. (Eds.) Metal Ions in Fungi. Marcel Dekker, New York, pp.1-38

Kosman, D.J., 2003. Molecular mechanisms of iron uptake in fungi. Molecular Microbiology 47, 1185-1197.

Kredics, L., Antal, Z., Manczinger, L., Nagy, E., 2001a. Breeding mycoparasitic *Trichoderma* strains for heavy metal resistance. Letters in Applied Microbiology 33, 112-116.

Kredics, L., Dóczi, I., Antal, Z., Mqanczinger, L., 2001b. Effect of heavy metals on growth and extracellular enzyme activities of mycoparasitic *Trichoderma* strains. Bulletin of Environmental Contaminant Toxicology 66, 249-254.

Kubicek, C.P., Harman, G.E., 1998. *Trichoderma* and *Gliocladium*: Basic Biology, Taxonomy and Genetics. Taylor & Francis, London, U.K.

Lee, B.N., Kroken, S., Chou, D.Y., Robbertse, B., Yoder, O.C., Turgeon, G.C., 2005. Functional analysis of all nonribosomal peptide synthetases in *Cochliobolus heterostrophus* reveals a factor, NPS6, involved in virulence and resistance to oxidative stress. Eukaryotic Cell 4, 545-555.

Leong, S., An, Z., 1997. Biosynthetic and regulatory aspects of siderophores. In: Winkelmann, G., Carrano, C.J. (Eds.) Transition Metals in Microbial Metabolism. Harwood, Amsterdam, The Netherlands, pp.51-79.

Liu, G., Greenshields, D.L, Sammynaiken, R., Hirji, R.N., Selvaraj, G., Wei, Y., 2007. Targeted alterations in iron homeostasis underlie plant defense responses. J. Cell Sci. 120, 596-605.

Madigan, M.T., Martinko, J.M., 2006. Brock Biology of Microorganisms. Benjamin Cummings, San Francisco.

Mei, B., Budde, A.D., Leong, S.A., 1993. *Sid1*, a gene initiating siderophore biosynthesis in *Ustilago maydis*: Molecular characterization, regulation by iron, and role in pathogenicity. Proc. Natl. Acad. Sci. USA 90, 903-907.

Mittler, R., Vanderauwera,S., Gollery,M., VanBreusegen, F., 2004. Reactive oxygen gene network of plants. Trends in Plant Science 9, 490-498.

Mukherjee, M., Hadar, R., Mukherjee, P.K., Horwitz, B.A. 2003. Homologous expression of a mutated beta-tubulin gene does not confer benomyl resistance on *Trichoderma virens.* Journal of Applied Microbiology 95, 861-867.

Oide, S., Moeder, W., Haas, H., Krasnoff, S., Gibson, D., Yoshioka, K.,Turgeon, B.G., 2006. NPS6, encoding a nonribosomal peptide synthetase involved in siderophore-mediated iron metabolism, is a conserved virulence determinant of plant pathogenic ascomycetes. The Plant Cell 18, 2839-2853.

Park,Y.H., Stack, J.P., Kenerley, C.M. 1992. Selective isolation and enumeration of *Gliocladium virens* and *G. roseum* from soil. Plant Disease 76, 230-255.

Philpott, C.C. 2006. Iron uptake in fungi: A system for every source. Biochim. Biophys. Acta 1763, 636-645.

Plattner, H.J., Diekmann, H., 1994. Enzymology of siderophore biosynthesis in fungi. In: Winkelmann, G., Winge, D.R.(Eds.) Metal Ions in Fungi. Marcel Dekker, New York, pp.99-117.

Renshaw, J.C., Robson, G.D., Trinci, A.P.J., Wiebe, M.G., Livens, F.R., Collison, D., Taylor, R.J., 2002. Fungal siderophores: Structures, functions, and applications. Mycological Research 106, 1123-1142.

Rogers, N.J., Carson, K.C., Glenn, A.R., Dilworth, M.J., Hughes, M.N., Poole, R.K., 2001. Alleviation of aluminum toxicity to *Rhizobium leguminosarum* bv. viciae by the hydroxamate siderophore vicibactin. Biometals 14, 59-66.

Samuels, G.J., 2006. *Trichoderma*: Systematics, the sexual state and ecology. Phytopathology 96, 195-206.

Santos, R., Buisson, N., Knight, S., Dancis, A., Comadro, J.M., Lesuisse, E., 2003 Haemin uptake and use as an iron source by *Candida albicans*: Role of CaHMX1-encoded haem oxygenase. Microbiology 149, 579-588.

Schippers, B., Bakker, A.W., Bakker, P.A.H.M., 1987. Interactions of deleterious and beneficial rhizosphere microorganisms and the effect of cropping practices. Annual Review of Phytopathology. 25, 339-358.

Schlesinger, W.H., 1997. Biogeochemistry. Academic Press, New York.

Schrettl, M., Bignell, E., Kragl, C., Joechl C., Rogers, T., Arnst, H.N. Jr., Haynes, K., Haas, H., 2004. Siderophore biosynthesis but not reductive iron assimilation is essential for *Aspergillus fumigatus* virulence. Journal of Experimental Medicine 200, 1213-1219.

Schrettl, M., Bignell, E., Kragl, C., Sabiha, Y., Loss, O., Eisendle, M., Wallner, A., Arnst Jr., H.N., Haynes, K., Haas, H., 2007. Distinct roles for intra- and extracellular siderophores during *Aspergillus fumigatus* infection. PLoS Pathogens 3, 1195-1207.

Singh, A., Srivastava, S., Singh, H.B., 2007. Effects of substrate on growth and shelf life of *Trichoderma harzianum* and its use in biocontrol of diseases. Bioresource Technology 98, 470-473.

Thomas, M.D., Kenerley,C.M., 1989. Transformation of the mycoparasite *Gliocladium*. Current Genetics 15, 415-420.

Turgeon, B.G., Oide, S., Bushley, K.E., 2007. Creating and screening *Cochliobolus heterostrophus* nonribosomal peptide synthetase mutants. Mycol. Res. 112, 200-206.

Van der Helm, D., Winkelmann, G., 1994. Hydroxamates and polycarboxylates as iron transport agents (siderophores) in fungi. In: Winkelmann, G., Winge, D.R.(Eds.) Metal Ions in Fungi. Marcel Dekker, New York, pp.39-98.

Van Loon, J.C., 2000. Induced resistance. In: Slusarenko, A.J., Fraser, R.S.S., Van Loon, J.C. (Eds.) Mechanisms of Resistance to Plant Diseases. Kluwer Academic Publishers, Dordrecht, The Netherlands, pp.521-574.

Vinale, F., Sivasithamparam, K., Ghisalberti, E.L., Marra, R., Woo, S.L., Lorito, M., 2008. *Trichoderma*-plant-pathogen interactions. Soil Biology and Biochemistry 40, 1-10.

Vogel, H.J., 1956. A convenient growth medium for *Neurospora* (medium N.) Microbiology and Genetics Bulletin 13,42-43.

Waters, B.M., Eide, D.J., 2002. Combinatorial control of yeast FET4 gene expression by iron, zinc and oxygen. J. Biol. Chem. 277, 33749-33757.

Wei X., Yang F., Straney D.C., 2005. Multiple non-ribosomal peptide synthetase genes determine peptaibol synthesis in *Trichoderma virens*. Can J Microbiol 51:423–429.

Wiest, A., Grzegorski, D., Xu, B., Goulard, C., DeLoan, S., Ebbole, D.J., Bodo, B., Kenerley, C., 2002. Identification of peptaibols from *Trichoderma virens* and cloning of a peptaibol synthetase. Journal of Biological Chemistry 277, 20862-20868.

Winkelmann, G., 2001. Siderophore transport in fungi. In: G.Winkelmann (Ed.), Microbial Transport Systems. Wiley-VCH, Weinheim, Germany, pp.463-479.

Winkelmann, G., 2007. Ecology of siderophores with special reference to the fungi. Biometals 20, 379-392.

Yedida, I., Benhamou, N., Chet, I., 1999. Induction of defense responses in cucumber plants (*Cucumis sativus L.*) by the biocontrol agent *Trichoderma harzianum*. Applied Environmental Microbiology 65, 1061-1070.

Yokoyama, T., Nakano, K., Zenki, M., 1999. Specific separation of nickel ion with bathophenanthroline disulfonic acid by capillary zone electrophoresis. Analytica Chimica Acta 396, 117-123.

Zhang, J., Mace, M.E., Stipanovic, R.D., Bell, A.A., 1993. Production and fungitoxicity of the terpenoid phytoalexins in cotton inoculated with *Fusarium oxysporum* f.sp. *vasinfectum*. Journal of Phytopathology 139, 247-252.

VITA

Name:	James Franklin Hurley IV
Address:	2132 TAMU, College Station, TX 77843-2132
Email Address:	laplata2006@tamu.edu
Education:	B.A., with triple major: Chinese, English, and Biology, University of Colorado at Boulder, 1997 M.S., Plant Pathology and Microbiology, Texas A&M University, 2009